

Selective Treg reconstitution during lymphopenia normalizes DC costimulation and prevents graft-versus-host disease

Holly A. Bolton, ... , Elena Shklovskaya, Barbara Fazekas de St. Groth

J Clin Invest. 2015;125(9):3627-3641. <https://doi.org/10.1172/JCI76031>.

Research Article

Immunology

Regulatory T cells (Tregs) have been shown to enhance immune reconstitution and prevent graft-versus-host disease (GVHD) after hematopoietic stem cell transplantation; however, it is unclear how Tregs mediate these effects. Here, we developed a model to examine the mechanism of Treg-dependent regulation of immune reconstitution. Lymphopenic mice were selectively reconstituted with Tregs prior to transfer of conventional CD4⁺ T cells. Full Treg reconstitution prevented the rapid oligoclonal proliferation that gives rise to pathogenic CD4 effector T cells, while preserving the slow homeostatic form of lymphopenia-induced peripheral expansion that repopulates a diverse peripheral T cell pool. Treg-mediated CTLA-4-dependent downregulation of CD80/CD86 on DCs was critical for inhibition of rapid proliferation and was a function of the Treg/DC ratio achieved by reconstitution. In an allogeneic BM transplant model, selective Treg reconstitution before T cell transfer also normalized DC costimulation and provided complete protection against GVHD. In contrast, cotransfer of Tregs was not protective. Our results indicate that achieving optimal recovery from lymphopenia should aim to improve early Treg reconstitution in order to increase the relative number of Tregs to DCs and thereby inhibit spontaneous oligoclonal T cell proliferation.

Find the latest version:

<https://jci.me/76031/pdf>



Selective Treg reconstitution during lymphopenia normalizes DC costimulation and prevents graft-versus-host disease

Holly A. Bolton,^{1,2} Erhua Zhu,^{1,2} Alexandra M. Terry,^{1,2} Thomas V. Guy,^{1,2} Woon-Puay Koh,¹ Sioh-Yang Tan,^{1,2} Carl A. Power,¹ Patrick Bertolino,¹ Katharina Lahl,³ Tim Sparwasser,⁴ Elena Shklovskaya,^{1,2} and Barbara Fazekas de St. Groth^{1,2}

¹T Cell Biology Laboratory, Centenary Institute of Cancer Medicine and Cell Biology, Camperdown, New South Wales, Australia. ²Discipline of Dermatology, Sydney Medical School, University of Sydney, Sydney, New South Wales, Australia. ³Institut für Medizinische Mikrobiologie, Immunologie und Hygiene, Technische Universität München, Munich, Germany. ⁴Institute of Infection Immunology, Centre for Experimental and Clinical Infection Research, Twincore, Hannover, Germany.

Regulatory T cells (Tregs) have been shown to enhance immune reconstitution and prevent graft-versus-host disease (GVHD) after hematopoietic stem cell transplantation; however, it is unclear how Tregs mediate these effects. Here, we developed a model to examine the mechanism of Treg-dependent regulation of immune reconstitution. Lymphopenic mice were selectively reconstituted with Tregs prior to transfer of conventional CD4⁺ T cells. Full Treg reconstitution prevented the rapid oligoclonal proliferation that gives rise to pathogenic CD4 effector T cells, while preserving the slow homeostatic form of lymphopenia-induced peripheral expansion that repopulates a diverse peripheral T cell pool. Treg-mediated CTLA-4-dependent downregulation of CD80/CD86 on DCs was critical for inhibition of rapid proliferation and was a function of the Treg/DC ratio achieved by reconstitution. In an allogeneic BM transplant model, selective Treg reconstitution before T cell transfer also normalized DC costimulation and provided complete protection against GVHD. In contrast, cotransfer of Tregs was not protective. Our results indicate that achieving optimal recovery from lymphopenia should aim to improve early Treg reconstitution in order to increase the relative number of Tregs to DCs and thereby inhibit spontaneous oligoclonal T cell proliferation.

Introduction

Achieving satisfactory immune reconstitution in lymphopenic subjects remains a major problem in many clinical settings, including following autologous or allogeneic hematopoietic stem-cell transplantation (HSCT) and recovery from cancer chemotherapy. Studies in both mouse and man have indicated that the lymphopenic state is associated with a spectrum of T cell abnormalities, including spontaneous proliferation, conversion to activated/memory phenotype, and tissue infiltration and damage (1–4). In addition, spontaneous proliferation is usually oligoclonal, leading to constriction of the T cell repertoire (5–8). Development of protocols that allow full reconstitution of the peripheral T cell compartment without inflammatory sequelae is an important aspect of ensuring good outcomes after lymphopenia-inducing therapeutic regimens.

Regulatory T cell infusion (Treg infusion) has been shown to promote immune reconstitution and reduce the incidence of graft-versus-host disease (GVHD) after allogeneic HSCT (9–17).

However, the mechanistic basis of this effect remains unclear. In mouse models in which the kinetics of CD4⁺ T cell lymphopenia-induced proliferation (LIP) have been studied in detail, 2 phases of lymphopenia-induced proliferation (LIP) have been identified (18, 19). The first is rapid, requires T cell receptor interactions (TCR interactions) with MHC-peptide ligands, and generates a differentiated effector cell population. Only 4%–6% of CD4⁺ T cells are subject to fast-phase LIP in syngeneic hosts (20). These spontaneously proliferating cells are believed to exhibit low affinity cross-reactivities with endogenous antigens, including self-antigens and gut microflora (21, 22), and their TCRs lie closest to the thymic cut-off for negative selection of self-reactive specificities. Although they represent a minor subpopulation, they rapidly generate a large oligoclonal population that dominates the reconstituted immune system and may induce tissue inflammation and autoimmunity. In contrast, slow-phase LIP is TCR independent, generates cells with a naive phenotype, and can be regarded as truly homeostatic, reconstituting a highly diverse polyclonal immune compartment. Previous studies have indicated that Tregs can partially suppress fast-phase proliferation (23). Importantly, a detailed quantitative study of the suppressive effect of selective Treg reconstitution on fast-phase proliferation has not previously been reported.

We have developed a mouse model to study the mechanism by which Tregs suppress LIP, based on reconstitution of syngeneic immunodeficient mice with pure populations of Tregs. Since Tregs are strictly IL-2 dependent but do not themselves make

Note regarding evaluation of this manuscript: Manuscripts authored by scientists associated with Duke University, The University of North Carolina at Chapel Hill, Duke-NUS, and the Sanford-Burnham Medical Research Institute are handled not by members of the editorial board but rather by the science editors, who consult with selected external editors and reviewers.

Conflict of interest: The authors have declared that no conflict of interest exists.

Submitted: June 12, 2015; **Accepted:** July 13, 2015.

Reference information: *J Clin Invest.* 2015;125(9):3627–3641. doi:10.1172/JCI76031.

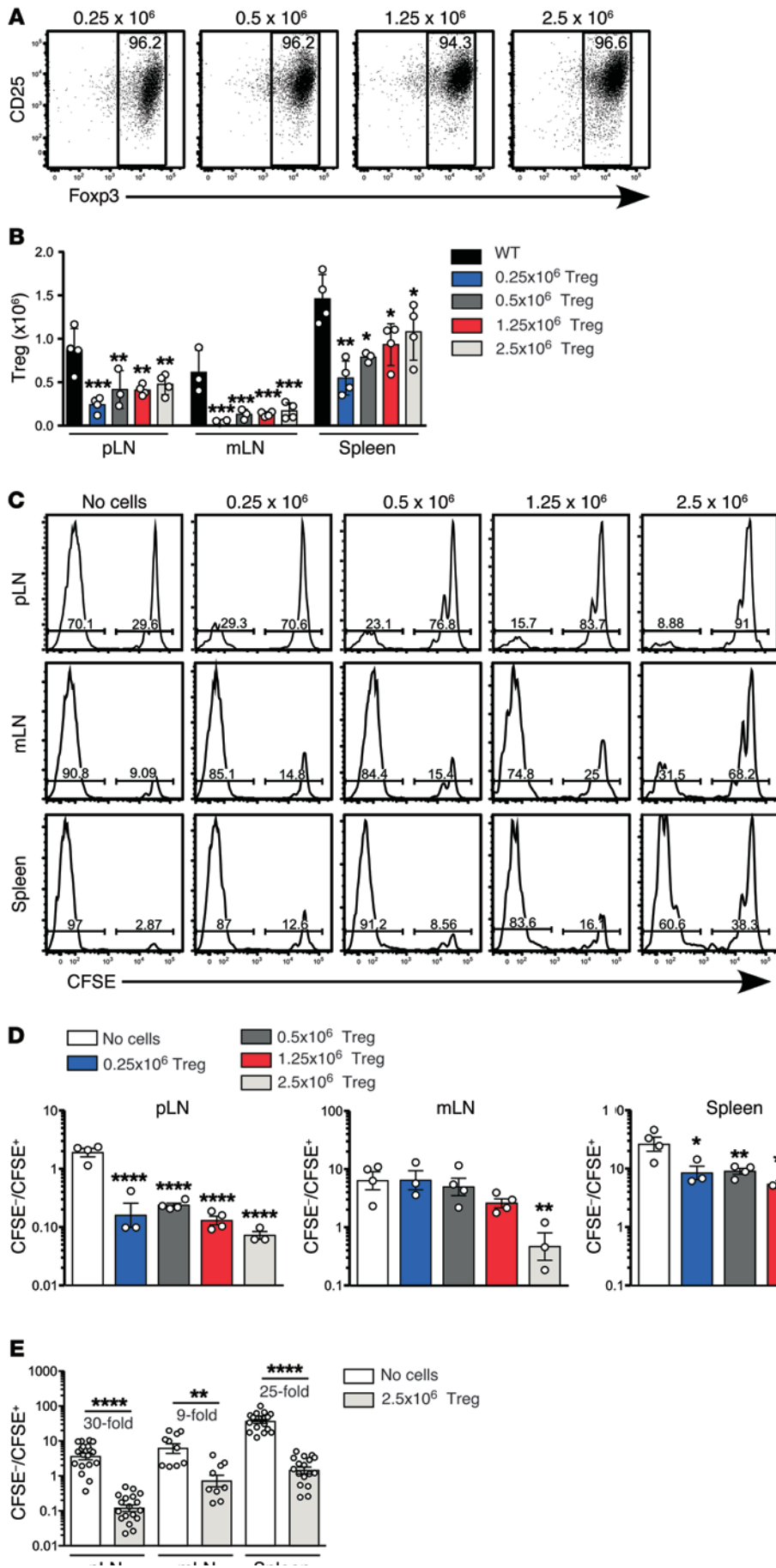


Figure 1. Effect on rapid-phase LIP of reconstitution of the Treg compartment prior to T cell transfer. Lymphopenic *Rag*^{-/-} mice were reconstituted with purified Tregs by adoptively transferring either 0.25 × 10⁶, 0.5 × 10⁶, 1.25 × 10⁶, or 2.5 × 10⁶ bead-selected CD4⁺CD25⁺ Tregs. Mice were treated with IL-2/JES6-1 complexes second daily to support Treg expansion. **(A)** Donor cells were distinguished from host cells by a CD45 allelic difference. Shown is expression of CD25 and Fopx3 on donor CD4⁺ T cells in pLN (*n* = 4 per group). **(B)** The total number of CD4⁺CD25⁺Fopx3⁺ Tregs was calculated for each Treg dose in pLN, mLN, and spleen of Treg-reconstituted mice, and for WT controls (*n* = 4 per group). Data in **A** and **B** are from a single experiment. The comparison of WT, *Rag*^{-/-} mice, and *Rag*^{-/-} mice reconstituted with 2.5 × 10⁶ CD4⁺CD25⁺ Tregs is representative of more than 10 independent experiments. **(C)** At day 7 after Treg transfer, 1 × 10⁶ CFSE-labeled CD4⁺CD25⁺ conventional T cells were adoptively transferred into unreconstituted or Treg-reconstituted *Rag*^{-/-} mice, as described for **A**. All mice were treated with second daily IL-2/JES6-1 complexes throughout the experiment. Representative CFSE division profiles of conventional CD4⁺ T cells are shown at 7 days after transfer (left panels). **(D)** The ratio of CFSE⁻ cells (>7 rounds of division) to CFSE⁺ T cells (0–3 rounds of division) was calculated. Data in **C** and **D** are from one experiment with *n* = 3–4 per group. **(E)** Comparison of the ratio of divided to undivided cells in the pLN, mLN, and spleen of unreconstituted or Treg-reconstituted *Rag*^{-/-} mice. Data are pooled from 6 independent experiments (*n* = 9–19 per group). Data in **B** and **D** were analyzed using one-way ANOVA with a Newman-Keuls post-test, while data in **E** were analyzed using a 2-tailed unpaired *t* test. Bars represent mean ± SEM with individual values indicated by the open circles. **P* < 0.05, ***P* < 0.01, and *****P* < 0.0001.

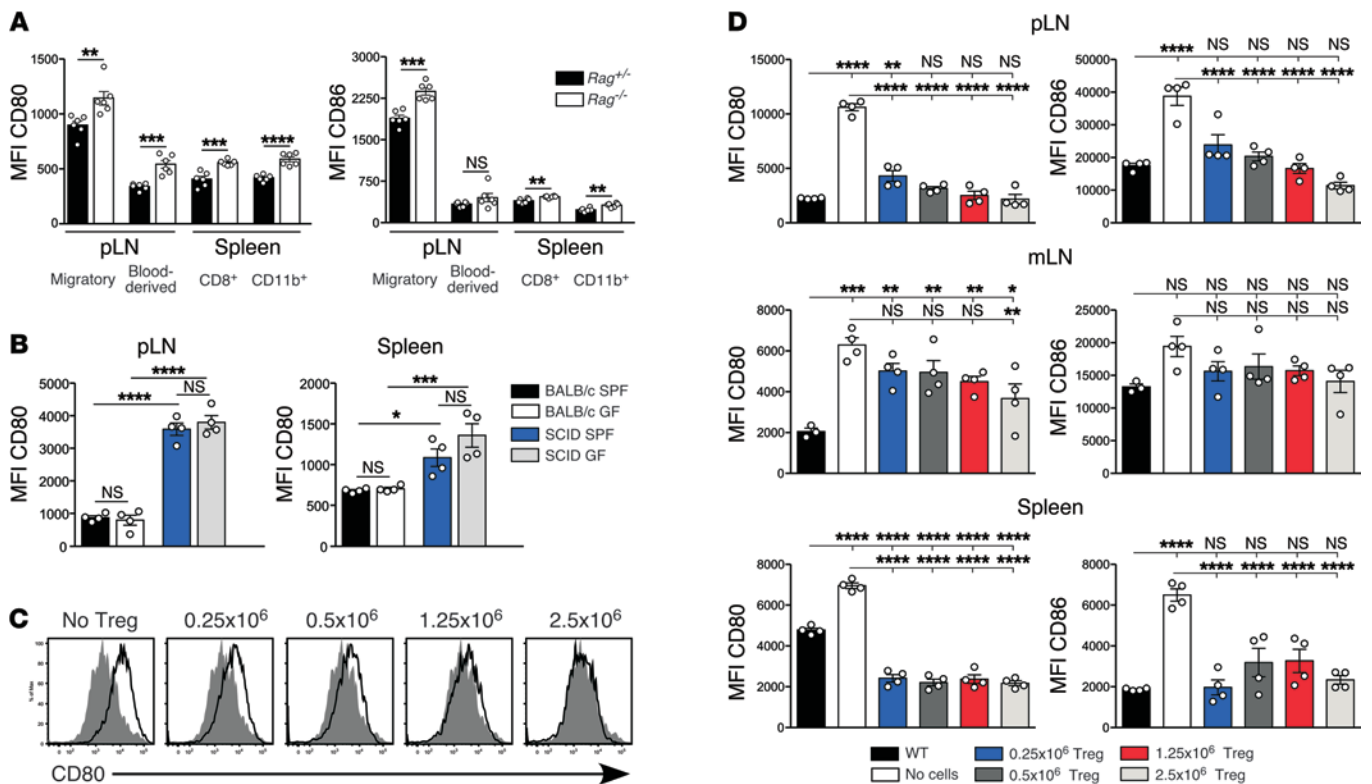


Figure 2. Expression of CD80 and CD86 by DCs from Treg-deficient mice. (A) MFI of CD80 (left panel) and CD86 expression (right panel) by DCs from immunodeficient *Rag*^{-/-} mice and their immunosufficient *Rag*^{-/-} littermates (*n* = 6 per group). Migratory DCs and blood-borne DCs in pLN/mLN were gated as MHCII^{hi}CD11c^{int} and MHCII^{int}CD11c^{hi}, respectively. Blood-borne DCs in the spleen were further subdivided based on expression of CD8 and CD11b. Results are from a single experiment and are representative of more than 20 independent experiments. (B) Comparison of DC phenotype in mice housed under SPF versus GF conditions. MFI of CD80 expression by CD11c^{hi}B220⁻ pLN and spleen DCs from immunosufficient BALB/c and immunodeficient C.B-17/lcr-scid mice housed under either SPF or GF conditions. Data are pooled from 2 independent experiments with 2 mice per group in each experiment. (C) Expression of CD80 by migratory DCs in the pLN of *Rag*^{-/-} mice that received either no cells or were reconstituted with 0.25 × 10⁶, 0.5 × 10⁶, 1.25 × 10⁶, or 2.5 × 10⁶ CD4⁺CD25⁺ Tregs (open histograms) compared with expression in untreated WT mice (shaded histograms). (D) Expression of CD80 (left panels) and CD86 (right panels) by migratory DCs in the pLN, mLN, and splenic DCs at day 7 after Treg reconstitution compared with expression in untreated WT and *Rag*^{-/-} mice. Data in C and D are from a single experiment with *n* = 4 per group. The comparison of WT, *Rag*^{-/-} mice, and *Rag*^{-/-} mice reconstituted with 2.5 × 10⁶ CD4⁺CD25⁺ Tregs is representative of more than 10 independent experiments. Data in A were analyzed using a 2-tailed *t* test, while data in B and D were analyzed using one-way ANOVA with a Newman-Keuls post-test. Bars represent mean ± SEM with individual values indicated by the open circles. **P* < 0.05, ***P* < 0.01, ****P* < 0.001, and *****P* < 0.0001.

IL-2, we used IL-2 complexes (24) to support reconstitution without the potentially confounding effects of cotransferred conventional T cells as an endogenous source of IL-2. Here, we show that Tregs prevent fast-phase LIP by downregulating the expression of costimulatory molecules by DCs, thereby allowing slow-phase LIP to proceed. In contrast, reconstitution with conventional CD4⁺ T cells further upregulates costimulation, enhances fast-phase LIP, and inhibits slow-phase LIP. The effect of Tregs is strictly dependent on the numerical ratio of Tregs to DCs in individual secondary lymphoid organs and requires expression of CTLA-4 by Tregs. Using a mouse model of allogeneic BM transplantation (BMT), we show that DC costimulation is also elevated following irradiation and can be reduced by means of reconstitution with either syngeneic or allogeneic Tregs. In addition, Treg reconstitution after BMT completely protected against development of GVHD, whereas cotransfer of Tregs and conventional T cells did not. Our results explain why clinical protocols favoring reconstitution of Tregs before conventional T cells may lead to superior long-term outcomes and suggest that ensuring adequate early Treg recon-

stitution is a crucial aspect of the management of lymphopenic patients. In addition, these findings may also explain the mechanistic basis behind the association of lymphopenia and autoimmunity, which has been noted in both mouse and man.

Results

Treg reconstitution inhibits spontaneous T cell proliferation in lymphopenic animals. To study the mechanism of Treg-dependent suppression of LIP, we developed a model in which pure populations of Tregs were adoptively transferred into immunodeficient *Rag*^{-/-} mice and provided with an exogenous source of IL-2 in the form of IL-2/anti-IL-2 mAb complexes (24). After 7 days, reconstituting Tregs were identified in lymph nodes (LN) and spleen by flow cytometry (Supplemental Figure 1; supplemental material available online with this article; doi:10.1172/JCI76031DS1). CFSE-labeling indicated that the vast majority of Tregs had proliferated after transfer (Supplemental Figure 2) and over 90% retained expression of FoxP3 in the peripheral LN (pLN) (Figure 1A), mesenteric LN (mLN), and spleen (Supplemental Figure 2). The degree

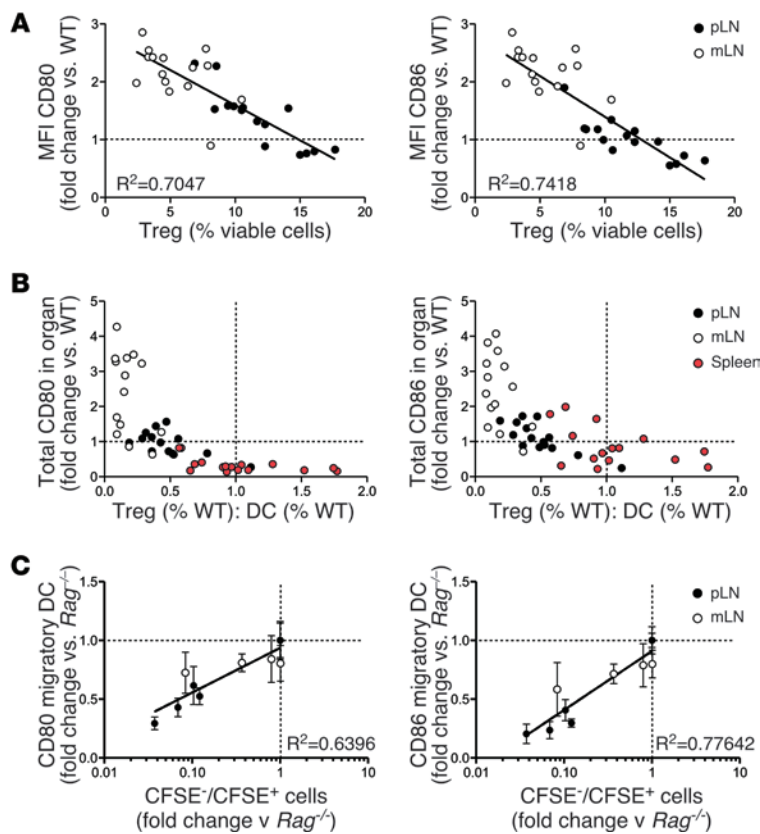


Figure 3. Correlation between Treg/DC ratio, DC costimulation, and spontaneous T cell proliferation. (A) MFI of CD80 and CD86 on migratory DCs in pLN (filled circle) and mLN (open circle) of *Rag*^{-/-} mice at day 7 after reconstitution with 0.25×10^6 , 0.5×10^6 , 1×10^6 , or 2.5×10^6 Treg ($n = 4$ per group). To allow for comparison between organs in which DCs express CD80/CD86 at different levels, expression of CD80/CD86 in individual pLN or mLN in Figure 2C was normalized against the mean WT expression level and then plotted against Treg frequency in the individual LN. A line of best fit with R^2 value is displayed. (B) To allow for comparison between organs in which both costimulation and DC number differed, total expression of CD80/CD86 in individual LN and spleen was calculated by multiplying MFI CD80 or CD86 by the number of DCs in the relevant organ and normalized against the WT mean. The Treg/DC ratio was also normalized against the WT mean ratio. (C) To compare expression of CD80/CD86 with the extent of fast-phase LIP, the ratio of CFSE⁻ (>7 divisions) to CFSE⁺ (0–3 divisions) T cells in the pLN and mLN at day 7 after transfer (Figure 1) was normalized against the ratio in *Rag*^{-/-} mice and plotted against migratory DC expression of CD80/CD86 (Figure 2, normalized against *Rag*^{-/-} expression) at the time of T cell transfer. A semilog curve with R^2 value is displayed. For A and B, broken lines indicate mean WT levels of costimulation/Treg/DC ratio, while in C, broken lines indicate mean *Rag*^{-/-} levels of costimulation/T cell proliferation.

of reconstitution varied according to transferred cell dose (0.25 , 0.5 , 1.25 , or 2.5×10^6 Tregs) and between different secondary lymphoid organs, being most efficient in spleen and least efficient in mLN (Figure 1B). To determine the effect of Treg reconstitution on fast-phase LIP, 1×10^6 CFSE-labeled CD4⁺CD25⁻ conventional T cells were adoptively transferred into reconstituted hosts on day 7, and the extent of proliferation was assessed after another 7 days. Proliferation was significantly inhibited in reconstituted hosts, with a trend toward increased inhibition at higher doses of Tregs (Figure 1, C and D). As with Treg reconstitution, the degree of inhibition also varied between the different lymphoid organs. A comparison of fast-phase LIP in *Rag*^{-/-} controls and *Rag*^{-/-} mice reconstituted with the highest dose of Tregs showed that inhibition was highest in the pLN (30-fold) and spleen (25-fold), compared with the mLN (9-fold) (Figure 1E), reflecting the differences in Treg-reconstitution efficiency in these organs (Figure 1B). In both untreated *Rag*^{-/-} controls and Treg-reconstituted mice, the relative number of divided cells was higher in spleen than in LN. This is likely due to preferential recirculation of divided effector T cells from LN to spleen, rather than reflecting the local rate of proliferation in the spleen itself.

Treg reconstitution reduces expression of CD80 and CD86 in lymphopenic animals. We next tested whether Treg reconstitution inhibited fast-phase LIP by downregulating expression of CD80 and CD86 by DCs, since CD28-CD80/CD86 signaling is known to be an absolute requirement for fast-phase LIP (19, 25). Tonic downregulation of DC costimulation by Tregs has been reported in vitro (26–29) but not in vivo. DCs from pLN, mLN, and spleen of untreated immunodeficient *Rag*^{-/-} mice consistently expressed

more CD80 and CD86 than those from immunosufficient *Rag*^{-/-} littermates (Figure 2A). These statistically significant increases, although relatively small, were seen in both MHCII^{hi}CD11c^{int} migratory and MHC^{int}CD11c^{hi} blood-derived DC populations, including both the CD8⁺ and CD11b⁺ splenic subsets. We excluded the possibility that elevated costimulation was due to subclinical microbial infection of *Rag*^{-/-} mice by showing that costimulatory molecules were equivalently elevated on DCs from immunodeficient mice housed under germ-free (GF) and specific pathogen-free (SPF) conditions (Figure 2B).

We next examined whether Treg reconstitution downregulated DC expression of CD80/CD86 in *Rag*^{-/-} mice. Preliminary experiments indicated that expression of CD80/CD86 was unaffected by the IL-2 treatment required to support Treg reconstitution (Supplemental Figure 3). DCs in Treg-reconstituted mice showed a uniform shift in surface expression of CD80/CD86, as illustrated for migratory DCs in the pLN (Figure 2C), indicating that comparing the mean fluorescent intensity (MFI) of CD80/CD86 expression provided a valid measure of the extent of downregulation. Splenic DCs and migratory DCs from pLN and mLN downregulated both CD80 and CD86 in response to Treg reconstitution (Figure 2D). In pLN, the extent of CD80/CD86 downregulation correlated with the number of Tregs transferred, with costimulation returning to WT levels only in mice that received at least 0.5×10^6 Tregs. In mLN, CD80 was significantly reduced only at the highest Treg cell dose (Figure 2D). To determine whether this difference could be explained by the comparatively poor Treg reconstitution in mLN (Figure 1B), we measured the correlation between Treg frequency and expression of CD80/CD86 on migratory DCs in individual

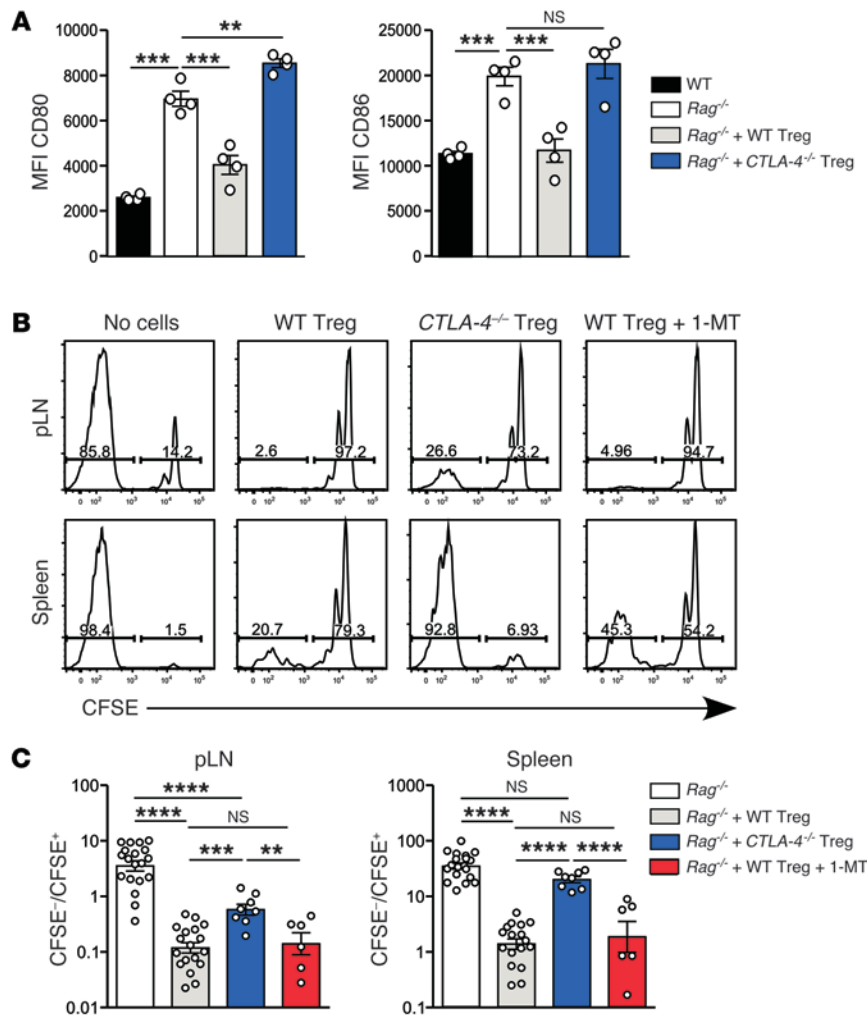


Figure 4. Effect of CTLA-4 expression by Tregs on modulation of CD80/CD86 and inhibition of fast-phase LIP. *Rag*^{-/-} hosts were reconstituted with flow-sorted WT or *Ctla-4*^{-/-} Tregs. *Ctla-4*^{-/-} and WT Tregs were purified from mixed BM chimeras generated with an 80:20 ratio of *Ctla-4*^{-/-}/WT BM. Fully reconstituted chimeras (>3 months after irradiation) were treated with IL-2/JES6-1 at -5, -4, and -3 days to expand Treg numbers before harvest at day 0. Treg reconstitution was performed as described in Figure 1. (A) MFI of CD80 (left) and CD86 (right) on migratory DCs from pLN (*n* = 4 per group). Bars represent mean ± SEM with individual values indicated by the open circles. Data are from 1 of 2 independent experiments. (B) 1 × 10⁶ CFSE-labeled WT polyclonal CD4⁺ T cells were transferred into *Rag*^{-/-} mice, either unreconstituted or reconstituted with WT or CTLA-4-deficient Tregs (*n* = 3 per group). All groups were treated with second daily IL-2/JES6-1 throughout the course of the experiment. One group of *Rag*^{-/-} mice reconstituted with WT Tregs received water supplemented with 5 mg/ml 1-MT from 3 days before CFSE-labeled cell transfer until organ harvest. Shown are representative CFSE division profiles from the pLN and spleen at day 7 after transfer. (C) The ratio of fully divided CFSE⁻⁷ T cells (>7 divisions) to CFSE⁺ T cells (0–3 divisions) within adoptively transferred CD4⁺ T cells was calculated for pLN and spleen, and summarized for all LIP experiments performed, totaling 6 independent experiments for *Rag*^{-/-} and WT Treg groups, 3 experiments with *Ctla-4*^{-/-} Tregs, and 2 experiments for 1-MT treatment (*n* = 6–19 per group). Statistical analysis was performed using one-way ANOVA with a Newman-Keuls post-test. ***P* < 0.01, ****P* < 0.001, *****P* < 0.0001.

pLN and mLN of Treg-reconstituted mice, using the data shown in Figure 2D. Because the steady-state levels of costimulation in pLN and mLN are different, costimulation data from each LN was normalized relative to the appropriate mean in WT mice. This analysis demonstrated a clear inverse correlation between Treg frequency and costimulation in individual LN (Figure 3A).

In the spleen, transfer of as few as 0.25 × 10⁶ Tregs reduced costimulation to WT levels (Figure 2D). This might reflect a more activated Treg phenotype in spleen as compared with LN, consistent with recent studies of BLIMP-reporter mice (30). However our data indicated that almost all Tregs in reconstituted *Rag*^{-/-} mice expressed a highly activated ICOS^{hi} phenotype, irrespective of site (Supplemental Figure 4A). A second possibility was that the effect of Tregs on costimulation within a particular organ was a function of the numerical ratio of Tregs to the DCs producing the costimulatory molecules. In this model, any change in DC numbers as a result of Treg reconstitution would impact on costimulation. Analysis of the experiment shown in Figure 2 indicated that DC numbers in spleen but not pLN were lower for all groups of Treg-reconstituted mice compared with WT controls (Supplemental Figure 4B). The splenic Treg/DC ratio was similar in Treg-reconstituted and WT mice, even at the lowest input Treg dose, whereas in pLN, even the

highest Treg dose failed to normalize the Treg/DC ratio (Supplemental Figure 4C). When the degree of Treg reconstitution was adjusted to reflect the Treg/DC ratio in individual lymphoid organs, an inverse relationship with total costimulation (MFI multiplied by DC number relative to WT) was apparent for all organs (Figure 3B). Normal levels of CD80 were achieved at approximately 50% of normal Treg/DC ratio in LN and spleen, consistent with the highly activated phenotype of reconstituting Tregs (Supplemental Figure 4A). We next correlated DC expression of costimulation at the time of T cell transfer with the rapid spontaneous T cell proliferative response shown in Figure 1. The size of the T cell response (indicated by the ratio of CFSE⁻⁷ cells [>7 divisions] to CFSE⁺ T cells [0–3 divisions]) in Treg-reconstituted *Rag*^{-/-} mice was normalized against *Rag*^{-/-} controls in order to allow comparison between organs in which baseline proliferation differed. This analysis was limited to pLN and mLN, since the spleen contains a mixture of T cells that have undergone activation and proliferation in situ and divided T cells that have migrated from other sites. When plotted against expression of CD80 and CD86 in Treg-reconstituted mice (also normalized against expression in *Rag*^{-/-} controls), a strong positive correlation between CD80/CD86 expression and T cell proliferation was observed (Figure 3C).

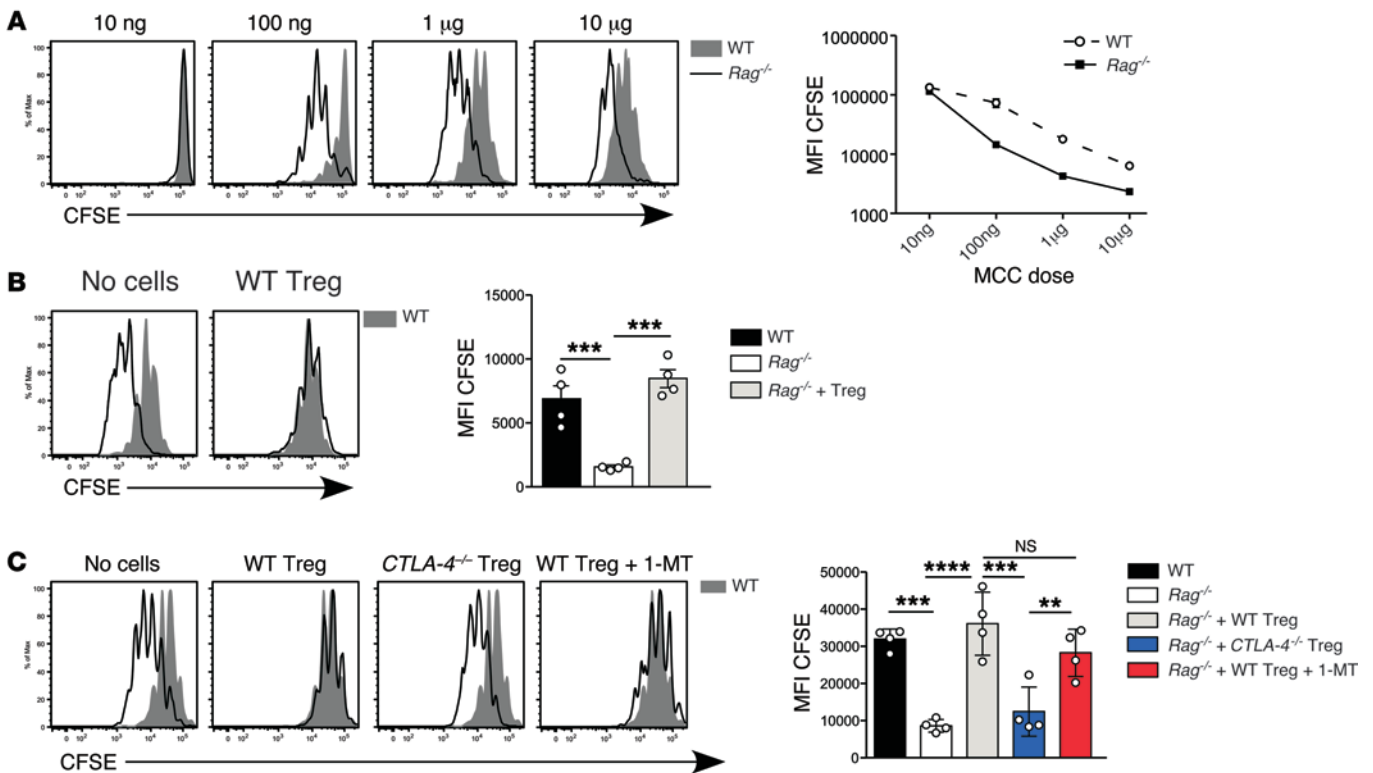


Figure 5. Effect of Treg reconstitution on naive T cell responses to specific antigen. (A) 1×10^6 5C.C7 TCR tg *Rag*^{-/-} T cells were adoptively transferred into WT or *Rag*^{-/-} mice, together with i.v. MCC peptide at the indicated doses. Left panel: Representative CFSE division profiles from the pLN at day 3 after transfer in WT (filled histograms) and *Rag*^{-/-} hosts (unfilled histograms) ($n = 3$ per group). Right panel: CFSE MFI on donor 5C.C7 T cells plotted against MCC dose in WT (broken line) and *Rag*^{-/-} hosts (unbroken line). Results are representative of 3 independent experiments. (B) 5C.C7 T cell proliferation in response to 1 μ g i.v. peptide in *Rag*^{-/-} hosts reconstituted with 2.5×10^6 WT Tregs. Left panel: Representative day 3 CFSE division profiles in pLN of Treg-reconstituted *Rag*^{-/-} hosts (unfilled histograms) and WT controls (filled histograms) ($n = 4$ per group). Right panel: CFSE MFI on 5C.C7 T cells. Data are representative of 3 independent experiments. (C) 1×10^6 CFSE-labeled 5C.C7 T cells were transferred into *Rag*^{-/-} hosts reconstituted with WT or CTLA-4-deficient Tregs ($n = 4$ per group). As described in Figure 4, one group of WT Treg-reconstituted mice was treated with 1-MT. MCC peptide (1 μ g) was administered i.v. at the time of T cell transfer. Left panel: CFSE division profiles in pLN at day 3 after T cell transfer (unfilled histograms) and untreated WT controls (filled histogram). Right panel: CFSE MFI on 5C.C7 T cells. Data are from 1 of 2 independent experiments for comparison of WT and CTLA-4-deficient Tregs, and a single experiment for 1-MT treatment. Statistical analysis of B and C was performed using one-way ANOVA with a Newman-Keuls post-test. Bars represent mean \pm SEM with individual values indicated by the open circles. ** $P < 0.01$, *** $P < 0.001$, **** $P < 0.0001$.

Taken together, these data suggest that, under steady-state conditions, the capacity of Tregs to control costimulation is a function of the ratio of Tregs to DCs. As the Treg/DC ratio drops below normal, costimulation increases and fast-phase LIP ensues as individual CD4⁺ T cells receive sufficient TCR/CD28-dependent stimulation to divide. Thus Tregs can be considered as a fail-safe against autoimmunity, backing up thymic negative selection of high-affinity self-reactivity by fine-tuning costimulation to control the peripheral T cell activation threshold.

CTLA-4 expression by Tregs is required for modulation of costimulation and fast-phase LIP. Treg-dependent downregulation of CD80/CD86 expression in vitro requires CTLA-4 (28, 29). To test whether Tregs also use CTLA-4 in vivo, we compared the function of CTLA-4-deficient and WT Tregs in reconstituted *Rag*^{-/-} mice. To generate populations of WT and CTLA-4-deficient Tregs with equivalent activation status at the time of adoptive transfer, we made mixed WT/CTLA-4^{-/-} BM chimeras in which the dominant effect of WT CTLA-4^{+/+} Tregs prevented the spontaneous activation and immunopathology present in CTLA-4^{-/-} mice (31). CTLA-4^{-/-} and WT Tregs isolated from these chi-

meras had comparable purity and Foxp3 expression levels (Supplemental Figure 5, A and B). Reconstitution of *Rag*^{-/-} hosts with CTLA-4-deficient Tregs failed to reduce expression of either CD80 or CD86 (Figure 4A). This was not due to suboptimal Treg reconstitution, as the number of Foxp3⁺ Tregs was higher in the CTLA-4-deficient group (Supplemental Figure 5C), most likely due to the absence of the cell-intrinsic CTLA-4-mediated negative signal. Involvement of CTLA-4 in Treg-dependent downregulation of CD80/CD86 expression, combined with the approximately 2-fold increase in CTLA-4 levels in reconstituting Tregs (Supplemental Figure 4A), may explain why only 50% of the normal number of Tregs was required to reduce costimulation to WT levels (Figure 3B).

Next, we assessed the extent to which fast-phase LIP was controlled by CTLA-4-dependent downregulation of costimulation. Compared with WT Tregs, CTLA-4-deficient Tregs were significantly impaired in their ability to inhibit fast-phase LIP in *Rag*^{-/-} mice (Figure 4, B and C), although some residual suppressive activity of CTLA-4-deficient Tregs was apparent, particularly in pLN. The mechanism mediating such residual suppres-

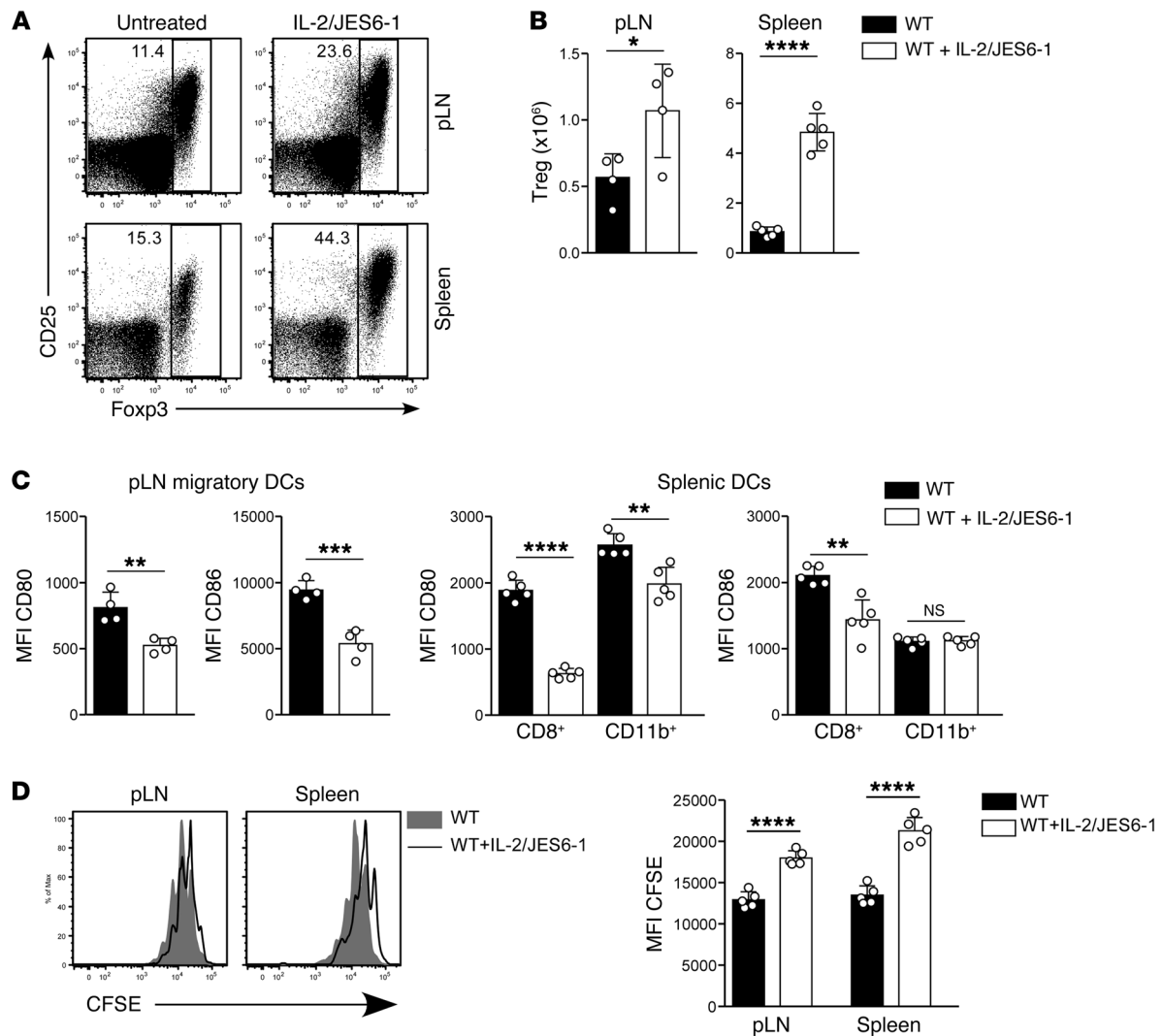


Figure 6. Effect of expansion of Treg populations in immunosufficient mice on DC costimulation and T cell proliferation. WT mice were treated with IL-2/JES6-1 complexes at days 0, 1, and 2, and lymphoid organs were harvested at day 5. **(A)** Representative plots of Foxp3 versus CD25 expression by CD4⁺ T cells from pLN and spleen. Numbers indicate the percentage of cells within the gate. **(B)** Absolute number of Foxp3⁺ Tregs in pLN and spleen of untreated versus IL-2/JES6-1-treated WT mice. **(C)** MFI of CD80 and CD86 expression by migratory DCs in pLN (left panels) and CD8⁺ and CD11b⁺ subsets of splenic DCs (right panels). Data in **A–C** are representative of 3 independent experiments with $n = 5$ per group. **(D)** Proliferation of adoptively transferred 5C.C7 T cells in response to 1 μ g i.v. peptide in WT hosts pretreated with IL-2/JES6-1 complexes at days -5, -4, and -3. Left panel: representative CFSE division profiles from pLN and spleen at day 3 after T cell transfer for IL-2/JES6-1 treated hosts (unfilled histograms) compared with untreated WT hosts (filled histograms). Right panel: MFI of CFSE expression by adoptively transferred 5C.C7 T cells ($n = 5$ mice per group). Data are from a single experiment. Statistical analysis of **B–D** was performed using 2-tailed unpaired t tests. Bars represent mean \pm SEM with individual values indicated by the open circles. * $P < 0.05$, ** $P < 0.01$, *** $P < 0.001$, and **** $P < 0.0001$.

sion in our model is currently unknown. However, our finding that deletion of a single molecule, CTLA-4, in Tregs simultaneously impaired their ability to control DC costimulation and to prevent fast-phase LIP supports a model in which downregulation of DC costimulation is a major mechanism used by Tregs to control fast-phase LIP.

We also tested whether CTLA-4-dependent induction of the immunomodulatory enzyme indoleamine 2,3-dioxygenase (IDO) was involved in Treg-dependent suppression, as previously reported (32, 33). Blocking IDO function by administering 1-methyl-DL-tryptophan (1-MT) (34) did not significantly impair Treg-dependent inhibition of fast-phase LIP (Figure 4, B and C), indicating no detectable role for IDO in our experimental model.

Treg reconstitution normalizes enhanced CD4⁺ T cell responses to foreign antigen. If Tregs mediate at least part of their suppressive function by downregulating costimulation, then they should also inhibit high-affinity responses. To test this, we substituted as a read-out the well-defined response of 5C.C7 TCR transgenic (tg) CD4⁺ T cells to their cognate antigen, moth cytochrome c (MCC) (35, 36). We predicted that higher constitutive expression of CD80/CD86 by DCs in unmanipulated *Rag*^{-/-} hosts (Figure 2A) should enhance the naive 5C.C7 T cell response, particularly at suboptimal antigen doses. 5C.C7 TCR tg T cells showed increased proliferation to MCC peptide ligand in *Rag*^{-/-} hosts compared with WT hosts, most pronounced at lower peptide doses (Figure 5A). Treg reconstitution reduced 5C.C7 proliferation to peptide in the pLN to the level seen in

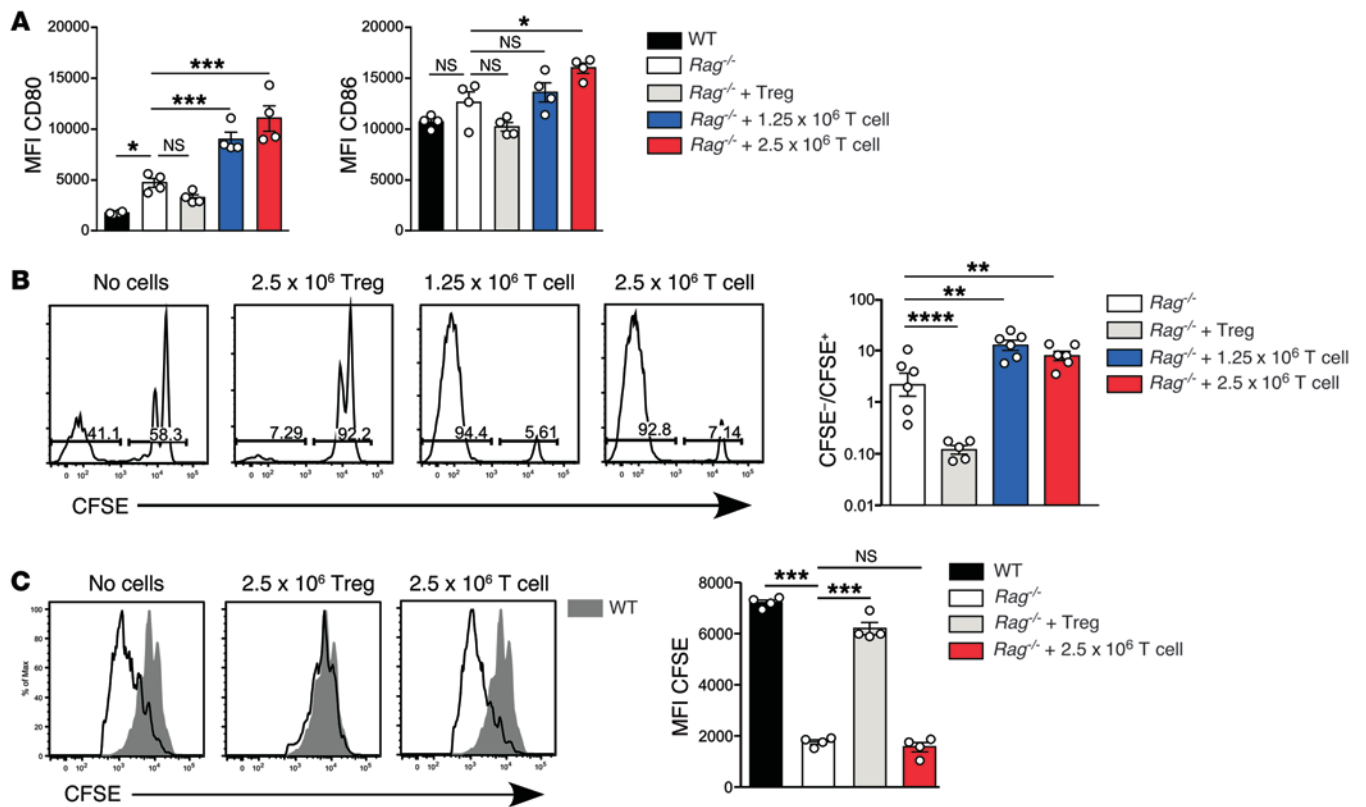


Figure 7. Effect of conventional T cell reconstitution on DC expression of CD80/CD86 and fast-phase LIP. (A) *Rag*^{-/-} mice were reconstituted with 2.5 × 10⁶ Tregs or naive conventional T cells at a dose of 1.25 × 10⁶ or 2.5 × 10⁶ (*n* = 4 per group). Naive conventional T cells were flow sorted as CD3⁺ CD4⁺ CD25⁻ CD38⁻ CD44⁻. Expression of CD80 (left panel) and CD86 (right panel) by migratory DCs in pLN is shown. Data are representative of 2 independent experiments. (B) 1 × 10⁶ CFSE-labeled polyclonal CD4⁺ T cells were transferred into unreconstituted, Treg-reconstituted, or conventional T cell–reconstituted *Rag*^{-/-} mice. Second daily IL-2/JES6-1 treatment was continued for all groups until lymphoid organ harvest 7 days after CFSE-labeled cell transfer. Adoptively transferred CD4⁺ WT T cells were identified based on differential expression of CD45 alleles. Left panel: Representative CFSE division profiles from the pLN day 7 after transfer. Right panel: Ratio of CFSE⁻ T cells (>7 divisions) to CFSE⁺ T cells (0–3 divisions) within adoptively transferred T cells was calculated (*n* = 6 per group). Data are pooled from 2 independent experiments. (C) Proliferation of adoptively transferred 5C.C7 T cells in response to 1 μg i.v. peptide in *Rag*^{-/-} hosts, either unreconstituted or reconstituted with 2.5 × 10⁶ Tregs or conventional T cells (*n* = 4 per group). Left panel: Representative CFSE division profiles in pLN of *Rag*^{-/-} hosts (unfilled histograms) compared with WT controls (filled histograms) 3 days after adoptive transfer of 5C.C7 T cells. Right panel: MFI of CFSE expression by adoptively transferred 5C.C7 T cells. Data are representative of 2 independent experiments. Statistical analysis of A–C was performed using one-way ANOVA with a Newman-Keuls post-test. Bars represent mean ± SEM with individual values indicated by the open circles. **P* < 0.05, ***P* < 0.01, ****P* < 0.001, and *****P* < 0.0001.

WT hosts (Figure 5B), consistent with the reduction in CD80/CD86 (Figure 2, C and D). This effect was abolished when *Rag*^{-/-} mice were reconstituted with CTLA-4–deficient Tregs (Figure 5C). Once again, inhibition of IDO had no effect on suppression by WT Tregs. Treg reconstitution similarly suppressed the 5C.C7 T cell response in the spleen but not in the mLN, consistent with the relatively low level of Treg reconstitution in the latter organ (not shown).

Steady-state regulation of DC costimulation by Tregs in immunosufficient mice. The data reported above indicate that Tregs downregulate CD80/CD86 expression during reconstitution of immunodeficient mice. To test whether they also downregulate costimulation in immunosufficient mice under steady-state conditions, we expanded Treg populations by administering IL-2 complexes to WT mice. IL-2 treatment increased Treg numbers (Figure 6, A and B) and concomitantly reduced expression of CD80 and CD86 (Figure 6C). After Treg expansion, antigen-specific T cell proliferation was also reduced (Figure 6D). Thus Tregs mediate tonic downregulation of costimulation under lymphosufficient and lymphopenic conditions.

Effect of conventional T cells on costimulation and fast-phase LIP. In the absence of Tregs, oligoclonal CD4⁺ T cells reconstitute the immune system by means of fast-phase LIP. To model the downstream effects of ongoing LIP and compare them to Treg reconstitution, we adoptively transferred *Rag*^{-/-} hosts with naive conventional CD4⁺ T cells and compared them to hosts reconstituted with 2.5 × 10⁶ Tregs. All host mice were administered IL-2 complexes during reconstitution. Because conventional T cells produced generally larger but more variable numbers of reconstituting cells than Tregs, irrespective of whether they were provided with exogenous IL-2 (Supplemental Figure 6), each experiment included groups reconstituted with either 1.25 × 10⁶ or 2.5 × 10⁶ conventional T cells to bracket the size of the reconstituted Treg population (not shown). In marked contrast to the effect of Tregs, both doses of conventional T cells upregulated expression of costimulation on DCs in pLN (Figure 7A) and spleen (not shown). These opposing effects of Tregs and conventional T cells on costimulation appear to be specific for CD80/CD86, as we observed minimal changes in

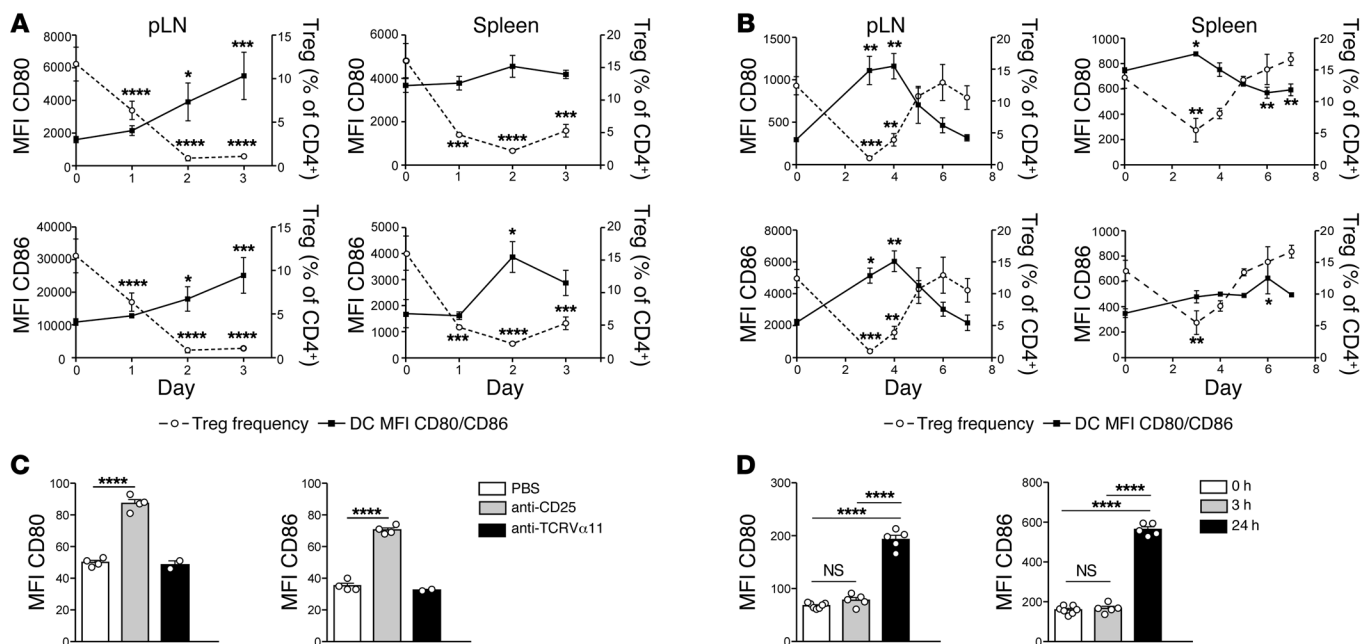


Figure 8. Effect of Treg depletion in immunosufficient animals on expression of costimulation. (A and B) DEREG mice were treated with 1 μ g DT i.p. at days 0 and 1. MFI of CD80 (upper panels) and CD86 expression (lower panels) by migratory DCs from pLN (left) or splenic DCs (right; unbroken lines) graphed against Tregs as a percentage of CD4⁺ T cells (dotted lines) between days 0 and 3 (A), and at days 0 and 3–7 (B). Data in A and B are mean \pm SEM ($n = 3$ –4 per group) and are each from a single experiment. (C) WT mice were treated with 500 μ g anti-CD25 (clone PC61) 18 hours before harvest of spleens. Controls received either PBS, or 500 μ g of anti-V α 11 (clone RR8) ($n = 2$ –4 per group). MFI of CD80 and CD86 expression by unfractionated CD11c⁺B220⁻ splenic DCs from a single experiment is shown. (D) WT mice were irradiated with 700 cGy, and spleens were harvested at 0, 3, or 24 hours. MFI of CD80 and CD86 expression by unfractionated CD11c⁺B220⁻ splenic DCs is shown ($n = 5$ –7 per group). Data are from a single experiment. Statistical analysis of A–D was performed using one-way ANOVA with a Newman-Keuls post-test. Bars represent mean \pm SEM with individual values indicated by the open circles. * $P < 0.05$, ** $P < 0.01$, *** $P < 0.001$, and **** $P < 0.0001$.

expression of other costimulatory molecules under the same conditions (Supplemental Figure 7). In addition to increasing expression of CD80/CD86, T cell reconstitution also significantly increased fast-phase LIP in both pLN (Figure 7B) and spleen (not shown), but had no effect on 5C.C7 T cell responses to specific peptide (Figure 7C), possibly because the antigen-specific T cells in unreconstituted *Rag*^{-/-} hosts were already proliferating at a maximal rate.

Effect of Treg depletion in immunosufficient mice. Spontaneous immune reconstitution from a state of partial lymphopenia is likely to proceed in the presence of a mixed Treg/conventional T cell compartment, with each population exerting their essentially opposing effects. To model this situation, we used DEREG (depletion of regulatory T cell) mice expressing the diphtheria toxin receptor (DT receptor) under the control of the FoxP3 promoter (37). After administration of 2 doses of 1 μ g DT on days 0 and 1, Treg frequency reached a minimum on day 2, while expression of CD80 and CD86 increased (Figure 8A and Supplemental Figure 8, A and B). The extent of CD80/CD86 upregulation on day 2 was similar to that seen previously in immunodeficient mice (Figure 2). Between days 2 and 4, a further increase in costimulation was seen, although Treg frequency was either stable or increased. This finding is consistent with a secondary, positive effect of conventional T cell activation in response to the earlier increase in costimulation (38). Treg frequency returned to normal by day 6, accompanied by a reciprocal decrease in expression of CD80 and CD86 (Figure 8B and Supplemental Figure 8, C and D). Similar early effects on costimulation were observed after Treg deple-

tion of WT mice using anti-CD25 mAb, which selectively targets Tregs (Figure 8C), and gamma irradiation, which acutely depletes lymphocytes (Figure 8D). Taken together, these data suggest that Tregs are continuously required to maintain the normal steady-state level of costimulation on peripheral lymphoid-tissue DCs and that, when Treg numbers are reduced, the resulting increase in costimulation triggers a wave of naive T cell activation that further increases costimulation via positive feedback on DCs.

Immune reconstitution via slow-phase homeostatic LIP. In addition to undergoing fast-phase LIP, adoptively transferred CD4⁺ T cells undergo a slower homeostatic form of CD28-independent, IL-7-dependent proliferation in immunodeficient hosts, producing 1 or 2 cell divisions within 7 days of adoptive transfer (19, 25). This type of homeostatic proliferation maintains a highly diverse T cell repertoire of naive cells (39, 40). In the experiment shown in Figure 7B, it appeared that reconstitution with conventional T cells, but not Tregs, inhibited slow-phase LIP. This was confirmed by analysis of T cell phenotype, which showed that the proportion of cells with a naive CD44^{lo}CD62L⁺ phenotype was lower in hosts reconstituted with conventional T cells compared with Tregs (Figure 9, A and B). In order to study the slow-phase LIP response in a more sensitive model, we examined spontaneous proliferation of T cells isolated from *Cd28*^{-/-} mice, which do not undergo fast-phase LIP (19, 25). Conventional T cells strongly inhibited slow-phase LIP, whereas Tregs had very little effect (Figure 9C), likely due to their lower expression of IL-7R (41). Thus, prior reconstitution with Tregs selectively inhibits fast-phase LIP without impair-

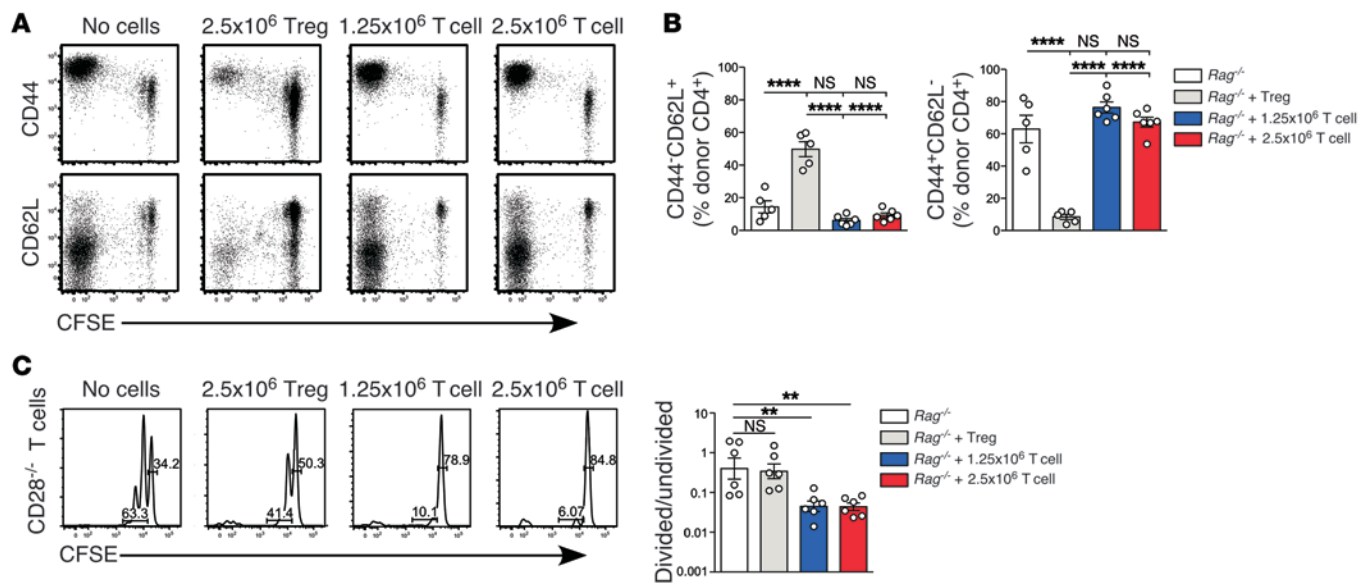


Figure 9. Effect of Treg reconstitution on homeostatic division of T cells retaining a naive phenotype. (A and B) 1×10^6 CFSE-labeled conventional CD4⁺CD25⁻ T cells were transferred into unreconstituted, Treg-reconstituted, or conventional T cell-reconstituted Rag^{-/-} mice. Expression of CD44 and CD62L on donor CD4⁺ T cells in the pLN ($n = 3$ per group). Data are representative of 2 independent experiments (A). The percentage of donor CD4⁺ T cells that were CD44⁺CD62L⁺ (left) and CD44⁺CD62L⁻ (right) was calculated ($n = 5-6$ per group). Data are pooled from 2 independent experiments (B). (C) 1×10^6 CFSE-labeled conventional CD4⁺CD25⁻ T cells from Cd28^{-/-} mice were adoptively transferred into unreconstituted, Treg-reconstituted, or T cell-reconstituted Rag^{-/-} mice. Representative CFSE division profiles from pLN at day 7 after transfer are shown (left panel). The ratio of slowly dividing cells (1-3 rounds of division at day 7) to undivided cells (0 rounds of division at day 7) was calculated (right panel) ($n = 6$ per group). Data are pooled from 2 independent experiments. Data in B and C were analyzed using one-way ANOVA with a Newman-Keuls post-test. Bars represent mean \pm SEM with individual values indicated by the open circles. ** $P < 0.01$ and **** $P < 0.0001$.

ing repopulation of the lymphoid pool via slow homeostatic proliferation, while conventional T cells in the absence of Tregs undergo fast-phase LIP, which in turn inhibits homeostatic division.

Treg reconstitution in a murine model of allogeneic BMT. Having demonstrated the effectiveness of Treg reconstitution in normalizing both DC costimulation and T cell responses in lymphopenic Rag^{-/-} mice, we next tested the relevance of these findings to BMT, in which the immune system reconstitutes a transiently lymphopenic environment produced by the BMT conditioning regimen. We performed allogeneic parent into F1 BMT, in which T cell depleted BM (TCD BM) from B10.BR mice was transplanted into lethally irradiated (C57BL/6 \times B10.BR)F1 mice (hereafter designated [B6.BR]F1). BMT recipients were reconstituted with either allogeneic donor-type Tregs (B10.BR) or syngeneic host-type Tregs ([B6.BR]F1). For Treg reconstitution, recipients were adoptively transferred with 2.5×10^6 Tregs at the time of BM transfer and treated second daily (on days 0, 2, 4, 6, and 8) with IL-2/JES6-1 complexes to support Treg survival and expansion, as described for Rag^{-/-} mice. Donor-derived Tregs could be clearly identified at day 7 after BMT in Treg-reconstituted mice but not in controls that received BM alone (Figure 10, A and B). Both allogeneic B10.BR and syngeneic [B6.BR]F1 Tregs were capable of reconstituting irradiated [B6.BR]F1 hosts. Mice that received BM alone contained a small population of residual host Tregs, which was not increased by treatment with IL-2/JES6-1 complexes.

The effect of Treg reconstitution on DC phenotype following BMT was then tested by examining migratory DCs in the pLN, which at day 7 after irradiation primarily consists of a radio-resistant population comprising Langerhans cells and a

small subset of dermal DCs (42, 43). The rapid increase in DC costimulation observed at 24 hours after irradiation (Figure 8D) was maintained at day 7 after BMT, with expression of CD80 and CD86 on pLN migratory DCs increasing by 4-fold and 3-fold, respectively, compared with DCs from nonirradiated controls (Figure 10C). Reconstitution with either B10.BR or [B6.BR]F1 Tregs reduced expression of both CD80 and CD86 to a level that did not significantly differ from nonirradiated WT controls. Consistent with the failure of IL-2/JES6-1 to increase the size of the residual Treg pool, treatment of irradiated BMT controls with IL-2/JES6-1 had no effect on expression of CD80/CD86 (Figure 10C). Expression of CD80/CD86 by DCs negatively correlated with Treg frequency for all treatment groups (Figure 10D), replicating the results in the Rag^{-/-} model.

Treg reconstitution following BMT protects against GVHD. Finally, we tested if Treg reconstitution and the associated reduction in costimulatory molecules limits CD4⁺ T cell-mediated GVHD in BMT recipients. Previous studies have demonstrated that cotransfer of purified Tregs at the time of T cell infusion can reduce GVHD, albeit with variable efficacy (10, 16, 44, 45). Published effects of cotransfer range from delay in disease onset to near complete protection against GVHD, depending on a variety of factors including number, activation status, and specificity of the transferred T cells. In one report, a 2-day delay in T cell administration after Treg transfer significantly improved survival (17).

We transferred 2.5×10^6 conventional CD4⁺CD25⁻ T cells from B10.BR donors into [B6.BR]F1 hosts on day 7 after irradiation, allowing time to achieve Treg reconstitution of BMT recipients prior to T cell transfer. Transfer of T cells into unreconsti-

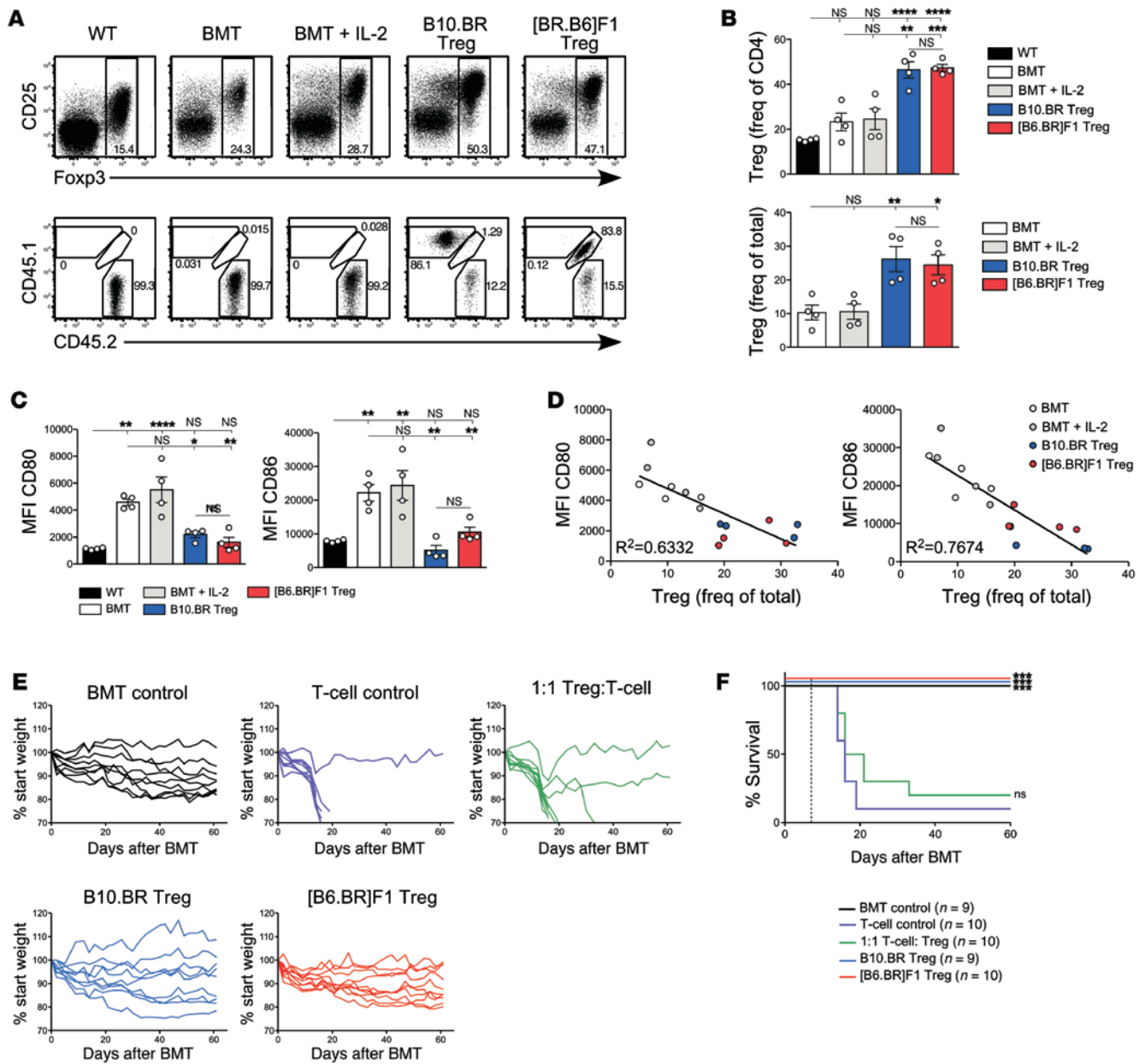


Figure 10. Effect of Treg reconstitution following BMT. (A) [B6.BR]F1 mice were lethally irradiated and transplanted with 5×10^6 TCD B10.BR BM cells. Mice received 2.5×10^6 CD4⁺CD25⁺ Tregs from B10.BR or [B6.BR]F1 donors at the time of BMT with IL-2/JES6-1 second daily. Controls included nonirradiated (WT) mice and irradiated mice that received BM alone (BMT) or BM and IL-2/JES6-1 (BMT + IL-2) ($n = 4$ /group). Top panel: Foxp3 and CD25 expression on total CD4⁺ T cells in pLN 7 days after BMT. Bottom panel: CD4⁺Foxp3⁺ Tregs were divided into host origin (CD45.2⁺), B10.BR donor origin (CD45.1⁺) and [B6.BR]F1 donor origin (CD45.1⁻/CD45.2⁻). (B) Foxp3⁺ Treg frequency of total CD4⁺ T cells (top panel), and total CD45-expressing cells (bottom panel). (C) Expression of CD80 (left) and CD86 (right) on pLN migratory DCs at day 7 after BMT. Bars represent mean \pm SEM with individual values indicated by open circles. * $P < 0.05$, ** $P < 0.01$, *** $P < 0.001$, and **** $P < 0.0001$. (D) MFI of CD80 (left panel) and CD86 (right panel) plotted against pLN Treg frequency among CD45-expressing cells. A line of best fit with R^2 value is displayed. Data in A–D are representative of 2 independent experiments. (E and F) BMT recipients were administered 2.5×10^6 B10.BR CD4⁺CD25⁺ T cells at day 7 after BMT. Groups included BMT recipients reconstituted with B10.BR or [B6.BR]F1 Tregs prior to T cell transfer, BMT recipients that received T cells alone, BMT recipients in which 1:1 B10.BR Tregs and T cells were cotransferred at day 7, and BMT recipients that did not receive T cells ($n = 9$ –10/group). Shown are mouse weights (E) and a Kaplan-Meier survival analysis (F). Data are pooled from 2 independent experiments.

tuted BMT recipients resulted in rapid, highly lethal GVHD in which mice failed to recover any of their irradiation-dependent weight loss (Figure 10E). The median survival of this group was 16 days after BMT, i.e., 9 days after T cell transfer (Figure 10F). Cotransfer of 2.5×10^6 allogeneic B10.BR Tregs at the time of T cell transfer (a 1:1 Treg/T cell ratio) had minimal protective effect

against GVHD development, possibly due to the severe disease in the B10.BR into [B6.BR]F1 model. Median survival was 18.5 days after BMT (11.5 days after T cell transfer) (Figure 10F) — not significantly different from the group that received T cells alone ($P = 0.20$). In contrast, Treg reconstitution prior to T cell transfer prevented GVHD in all animals, regardless of whether

transferred Tregs were allogeneic donor type (B10.BR) or syngeneic host type ([B6.BR]F1). Mice reconstituted with Tregs (either allogeneic or syngeneic) prior to T cell transfer showed similar weight changes to those in controls that received BMT but no T cell transfer (Figure 10E). Importantly, no deaths were recorded in Treg-reconstituted mice (Figure 10F). It should be noted that mice with high starting weights but no GVHD typically recovered to only 85%-90% of their preirradiation weight (Supplemental Figure 9A). The 100% survival rate in Treg-reconstituted mice represented a highly significant improvement to survival when compared with the Treg/T cell cotransfer protocol ($P = 0.0009$ for B10.BR Treg reconstitution, $P = 0.0005$ for [B6.BR]F1 Treg reconstitution). The protective effect was not due to IL-2/JES6-1 treatment of Treg-reconstituted mice, as second daily IL-2/JES6-1 treatment failed to prolong survival in the absence of Treg cell-reconstitution (Supplemental Figure 9, B and C).

Discussion

A major consideration in clinical settings of lymphopenia is the importance of achieving adequate immune reconstitution while avoiding complications due to oligoclonal T cell proliferation. The peripheral T cell pool expands to a greater size and expresses a more diverse TCR repertoire when Tregs are present during early immune reconstitution (5, 14, 39). Additionally, therapies that augment Treg numbers during lymphopenia have been demonstrated to be beneficial for the prevention of GVHD (9-16). However, it is not clear how Tregs mediate these beneficial effects.

Here, we have developed a mouse model to examine how Tregs control immune reconstitution. Using this model, we demonstrated that reconstitution of the Treg compartment prior to T cell transfer prevented rapid-phase proliferation of potentially pathogenic T cells, without impairing the slow-phase homeostatic form of LIP. In contrast, reconstitution with conventional CD4⁺ T cells enhanced subsequent fast-phase LIP and inhibited slow-phase immune reconstitution. Our data identify DC overexpression of the costimulatory molecules CD80/CD86 as the major driving force behind the fast-phase proliferative response in lymphopenia. The strong correlation between Treg cell number, DC expression of CD80/CD86, the extent of fast-phase LIP, and the magnitude of antigen-specific T cell responses in immunodeficient mice led us to hypothesize that Tregs play a critical role in controlling the steady-state level of DC costimulation under physiological conditions. We tested this function of Tregs in immunosufficient mice by demonstrating a similar relationship between Treg number and DC expression of CD80/CD86 following transient expansion or depletion of Tregs (summarized in Supplemental Figure 10). Deletion of a single molecule, CTLA-4, simultaneously impaired the ability of Tregs to control DC costimulation and prevent fast-phase LIP, supporting a model in which the 2 functions of Tregs are mechanistically linked. Our results indicate that CTLA-4-dependent downregulation of DC costimulation is a major mechanism used by Tregs to regulate the peripheral T cell-activation threshold. However, additional mechanisms must also be involved, particularly in LN where CTLA-4-deficient Tregs were still able to partially suppress fast-phase LIP. Finally, and most importantly for the potential application of our findings in clinical practice, we demonstrated

that our findings in lymphopenic *Rag*^{-/-} hosts were relevant to mice undergoing BMT, with Treg reconstitution similarly capable of mediating downregulation of CD80/CD86 and providing full protection against CD4⁺ T cell-mediated GVHD.

Our findings extend published data showing a CTLA-4-dependent reduction in expression of costimulatory molecules on DCs cocultured with Tregs (26-29) by demonstrating that CTLA-4 is also responsible for downregulation of CD80 and CD86 on DCs under steady-state conditions in vivo. Both secreted and cell-surface forms of CTLA-4 have been implicated in regulation of DC costimulation in vitro (46, 47), and cell-surface CTLA-4 expressed by high affinity conventional T cells was demonstrated to capture and internalize its ligands in vivo, a process termed transendocytosis. Whether Tregs also use transendocytosis in vivo is not yet known.

In our experiments, DC expression of CD80/CD86 was highly correlated with the ratio of Treg to DC. Our finding of the importance of the Treg/DC ratio is consistent with published studies in a variety of models in which induction of nonspecific CD4⁺ T cell lymphopenia leads to autoimmunity, despite a normal ratio of Tregs to conventional T cells (48-51). Our data suggest that immune reconstitution following cytoablative therapy is likely to benefit from early Treg reconstitution to normalize the ratio of Tregs to DCs, irrespective of the Treg/T cell ratio (2, 10). Indeed, in a murine model of GVHD, infusion of suboptimal Treg numbers was more effective at inhibiting GVHD if conventional T cell transfer was delayed by 2 days (17).

Recently, several studies have demonstrated that certain cytoablative treatments preferentially deplete conventional T cells, leaving Treg populations relatively intact (52, 53). Tregs are relatively resistant to cyclophosphamide, and the effectiveness of this treatment in preventing GVHD is critically dependent upon the presence of Tregs (52, 54). Additionally, treatment with anti-thymocyte globulin (ATG) preferentially depletes conventional T cells and, in low doses, actually promotes Treg expansion (53, 55). The mechanism by which such expansion inhibits GVHD (52) and promotes transplant tolerance (53) remains undetermined, but our results indicate that such an effect could readily be explained via Treg-dependent reduction in DC costimulation, thus limiting the activation of pathogenic T cells. Additionally, our results predict that early support for Treg reconstitution will be most crucial in patients receiving myeloablative conditioning rather than reduced-intensity conditioning, consistent with a recent report correlating Treg numbers and GVHD incidence after different conditioning for HSCT (13).

Our results suggest that specific targeting of the mechanisms supporting rapid-phase LIP, independent of Treg reconstitution, may also improve clinical outcomes for patients with transient lymphopenia. One possible agent is CTLA-4-Ig, which blocks recognition of CD80/CD86 and has been shown to promote transplant acceptance when combined with ATG therapy (53). In addition, treatments that favor slow-phase over fast-phase LIP may also help to achieve complete immune reconstitution. For example, IL-7 treatment preferentially enhances slow-phase LIP while inhibiting fast-phase proliferation (56, 57), and has been shown to promote faster immune reconstitution without enhancing GVHD (58).

In stark contrast, antitumor responses may benefit from conditions favoring fast-phase LIP during immune reconstitution (59). In general, antitumor responses in mouse (60) and man (61) are enhanced by a reduction in absolute Treg numbers and thus the Treg/DC ratio. In contrast, the graft-versus-leukemia response is maintained in the presence of Tregs, suggesting that it may be of higher affinity and thus less sensitive to deprivation of costimulatory drive (11, 62). However, Treg-depleting strategies come at a cost to TCR diversity and the size of the peripheral lymphocyte pool (5, 11, 14, 39), impairing responses to foreign pathogens such as listeria (39) and MCMV (14). A contributing factor to this impairment appears to be autoimmune damage to sites of T cell expansion, namely pLN, spleen, and thymus (14).

Finally, in addition to their implications for immune reconstitution in patients with iatrogenic lymphopenia, our results may also be of relevance in understanding the initiation of autoimmunity. In particular, the importance of the Treg/DC ratio in maintaining steady-state DC costimulation could explain the paradoxical link between autoimmunity and lymphopenia observed in animal models (48–51) and in several human immunodeficiency states (63).

Methods

Mice. All mice were bred and housed under SPF conditions in the Centenary Institute Animal Facility, apart from BALB/cWehi and C.B-17/lcr-scld animals raised under GF or SPF conditions at the Walter & Eliza Hall Institute SPF Unit (Kew, Australia). *Rag-1*^{-/-} mice (64) were originally a gift from Lynn Corcoran (Walter & Eliza Hall Institute, Parkville, Australia). *Rag-2*^{-/-} mice (65) were purchased from Taconic Biosciences Inc. DEREK mice (37) were provided by Stephen Alexander (Children's Hospital, Westmead, Australia). Tg mice expressing the 5C.C7 TCR specific for the COOH-terminal epitope of MCC (35, 36) were bred on a *Rag-2*^{-/-} background. *Cd28*^{-/-} mice were originally purchased from The Jackson Laboratory. *Ctla4*^{-/-} mice (66) obtained from Jim Allison (MD Anderson Cancer Center, Houston, Texas, United States) were maintained as homozygotes on *Rag-1*^{-/-} and *Rag-2*^{-/-} backgrounds. F1 crosses were performed to generate immunosufficient (*Rag-1*^{-/-}*Rag-2*^{-/-}) *Ctla4*^{-/-} BM donors. Experimental mice were >8 weeks of age, with the exception of *Ctla4*^{-/-} BM donors, which were used at 2–3 weeks of age due to early-onset lymphoproliferative disease in these mice.

Reconstitution of lymphopenic mice. Tregs for reconstitution were purified by 2-step magnetic bead enrichment of single-cell suspensions prepared from pooled peripheral and mesenteric LN and spleens. Step 1 involved staining with a mixture of hybridoma supernatants (anti-B220 [RA3.6B2], anti-CD8α [53-6.7], anti-CD11b [M1/70], and anti-erythroid lineage [Ter119]) (Centenary Institute) detected with anti-rat microbeads (Miltenyi Biotec), followed by negative selection to enrich for CD4⁺ T cells. In step 2, CD25-expressing Tregs were positively selected by staining with anti-CD25-PE (BD Biosciences) followed by anti-PE MACS beads (Miltenyi Biotec). FoxP3 was expressed by 90%–95% of the CD4⁺CD25⁺ population. Naive conventional T cells for reconstitution were purified from the bead-enriched CD4⁺ population by flow cytometric sorting for CD4⁺CD38⁻CD44⁻ cells using an AriaII digital flow sorter (BD Biosciences). Treg contamination was <1%. Purified CD4⁺CD25⁺ Tregs or conventional CD4⁺CD38⁻CD44⁻ cells from WT mice were adoptively

transferred into syngeneic *Rag-1*^{-/-} or *Rag-2*^{-/-} hosts and expanded by second daily treatment with IL-2/JES6-1 complexes (24), consisting of 1 μg IL-2 complexed to 5 μg JES6-1 mAb.

T cell responses. For LIP, the bead-selected CD4⁺CD25⁻ population was CFSE labeled (5 × 10⁷ cells/ml in RPMI + 1% FCS, 5 mM CFSE for 5 minutes at 37°C) and 1 × 10⁶ cells were injected i.v. into syngeneic hosts. For antigen-specific T cell responses, pLN cells from 5C.C7 TCR tg *Rag-2*^{-/-} mice were CFSE labeled and 1 × 10⁶ CD4⁺ T cells were adoptively transferred into syngeneic hosts together with i.v. MCC peptide (residues 86–103). Where indicated,IDO was inhibited by the addition of 1-MT (Sigma-Aldrich) to drinking water at a concentration of 5 mg/ml, as previously described (34).

Manipulation of Treg number in immunosufficient mice. Tregs were expanded in WT mice by administering IL-2/JES6-1 at days 0, 1, and 2 before analyzing Treg number and DC phenotype on day 5. Tregs were depleted in DEREK mice by i.p. injection of 1 μg DT (Sigma-Aldrich) on days 0 and 1 (67). Alternatively, Tregs were depleted in WT mice by i.p. injection of 500 μg anti-CD25 mAb (clone PC61) 18 hours prior to organ harvest. Controls received either 500 μg anti-TCRVα11 mAb (clone RR8) or PBS (Centenary Institute). For radiation-induced depletion of lymphocytes including Tregs, mice were irradiated with 700 cGy and lymphoid organs were harvested 3 or 24 hours later.

Generation and purification of CTLA-4-deficient Tregs. CTLA-4 mixed BM chimeras were generated by irradiating CD45.1^{+/+} WT host mice with 2 × 600 cGy 24 hours prior to adoptive transfer of 5 × 10⁶ BM cells (4 × 10⁶ CD45.1^{+/+}.2⁺ *Ctla4*^{-/-} plus 1 × 10⁶ CD45.2^{+/+} WT). After reconstitution for >3 months, Treg numbers were boosted by administration of IL-2/JES6-1 at days 0, 1, and 2 before lymphoid organ harvest on day 5. CD4⁺ T cells were enriched by one round of negative bead selection, as detailed above, and then flow sorted for CD4⁺CD25⁺ cells expressing CD45.1^{+/+}.2⁺ (*Ctla4*^{-/-}) or CD45.2^{+/+} (WT).

BMT and development of GVHD. [B6.BR]F1 hosts were lethally irradiated with 1,200 cGy (given as a split-dose of 2 × 600 cGy separated by 3 hours) 24 hours prior to adoptive transfer of 5 × 10⁶ BM cells from B10.BR donors. BM cells were TCD prior to transfer by magnetic bead depletion of T cells stained with hybridoma supernatants (anti-Thy1.2 and/or a mixture of anti-CD4 [GK1.5] and anti-CD8α [53-6.7]) and detected with anti-rat microbeads (Miltenyi Biotec). To reduce the incidence of postirradiation coagulopathy due to suspected vitamin K deficiency, mice were routinely treated with 1 mg vitamin K on day 1 prior to irradiation, and at 3 and 7 days after irradiation. Treg reconstitution was performed by transferring 2.5 × 10⁶ B10.BR or [B6.BR]F1 CD4⁺CD25⁺ Tregs at the time of BM transfer and treating with IL-2/JES6-1 complexes at days 0, 2, 4, 6, and 8. GVHD was induced by transfer of 2.5 × 10⁶ CD4⁺CD25⁻ T cells 7 days after BM transfer. GVHD monitoring consisted of weighing 2–3 times per week, plus visual monitoring for activity, posture, fur texture, and skin integrity as previously described (68). Mice were euthanized if visual signs of GVHD were present and weight loss exceeded 15%, or if total weight loss reached 25%.

FACS analysis. For analysis of T cells, single-cell suspensions were prepared from pLN, mLN, or spleen. For analysis of DCs, organs were first enzymatically digested in 2 mg/ml collagenase IV (Sigma-Aldrich). mAbs used for cell-surface staining were all from BD Biosciences, apart from CD45.1 (clone A20, Centenary Institute), CD45.2 (clone 104, eBioscience), and GARP (clone F011-5, BioLegend). Intracellular staining for Foxp3 was performed using a murine Foxp3

staining kit (eBioscience) and anti-Foxp3 mAb (clone FJK-16s, eBioscience). Cells were analyzed using CantoII, LSRII, or LSRFortessa digital flow cytometers (all BD Biosciences). Data analysis was performed using FlowJo software (Tree Star Inc.).

Statistics. Statistical analysis was performed using GraphPad Prism version 5.0d. When comparing 2 groups, a 2-tailed unpaired *t* test was performed. Comparison of multiple groups was performed using one-way ANOVA with a Newman-Keuls post-test. Statistical analysis of cell-division ratios was performed on log-transformed data. Analysis of Kaplan-Meier survival curves was performed using a log-rank test with a Gehan-Breslow-Wilcoxon post-test. *P* values < 0.05 were considered significant.

Study approval. All experiments were performed with the consent of the University of Sydney or Sydney Local Health District Animal Ethics Committee.

Acknowledgments

We thank Kylie Webster and Jonathan Sprent (Garvan Institute, Sydney, Australia) for their advice regarding IL-2/JES6-1 expansion of Tregs. We thank Adrian Smith, Steven Allen, Suat Dervish, and Frank Kao for expert technical assistance with flow cytometric sorting, and Yik Wen Loh, David Hancock, and Suzanne Asad for technical assistance with experiments. This work was supported by Project Grants 000358, 000359, 1012930, 1012522, 1012544, and 1051843, as well as Program Grants 183700 and 427620, from the National Health and Medical Research Council of Australia. H.A. Bolton, A.M. Terry, and T.V. Guy were funded by Australian Postgraduate Awards; S.-Y. Tan by an International Postgraduate Research Scholarship; and W.-P. Koh by the National University

of Singapore. P. Bertolino was funded by a University of Sydney U2000 Postdoctoral Research Fellowship. B. Fazekas de St. Groth was funded by an NHMRC Research Fellowship.

Address correspondence to: Barbara Fazekas de St. Groth, Centenary Institute of Cancer Medicine and Cell Biology, Locked Bag No. 6, Newtown, New South Wales, 2042, Australia. Phone: 61.2.9565.6137; E-mail: b.fazekas@centenary.org.au.

Woon-Puay Koh's present address is: Duke-NUS Graduate Medical School Singapore, Singapore.

Sioh-Yang Tan's present address is: Immune Imaging Laboratory, Centenary Institute of Cancer Medicine and Cell Biology, Camperdown, New South Wales, Australia.

Carl A. Power's present address is: Mark Wainwright Analytical Centre, University of New South Wales, Randwick, New South Wales, Australia.

Patrick Bertolino's present address is: Liver Immunology Laboratory, Centenary Institute of Cancer Medicine and Cell Biology, Camperdown, New South Wales, Australia.

Katharina Lahl's present address is: Laboratory of Immunology and Vascular Biology, Department of Pathology, Stanford University School of Medicine, Stanford, California, USA. Or: The Center for Molecular Biology and Medicine, Veterans Affairs Palo Alto Health Care System, Palo Alto, California, USA.

- Jameson SC. T cell homeostasis: keeping useful T cells alive and live T cells useful. *Semin Immunol.* 2005;17(3):231-237.
- Krupica T Jr, Fry TJ, Mackall CL. Autoimmunity during lymphopenia: a two-hit model. *Clin Immunol.* 2006;120(2):121-128.
- Chinen T, Volchkov PY, Chervonsky AV, Rudensky AY. A critical role for regulatory T cell-mediated control of inflammation in the absence of commensal microbiota. *J Exp Med.* 2010;207(11):2323-2330.
- Daikeler T, Tyndall A. Autoimmunity following haematopoietic stem-cell transplantation. *Best Pract Res Clin Hematol.* 2007;20(2):349-360.
- Mackall CL, Bare CV, Granger LA, Sharrow SO, Titus JA, Gress RE. Thymic-independent T cell regeneration occurs via antigen-driven expansion of peripheral T cells resulting in a repertoire that is limited in diversity and prone to skewing. *J Immunol.* 1996;156(12):4609-4616.
- Gorski J, et al. Circulating T cell repertoire complexity in normal individuals and bone marrow recipients analyzed by CDR3 size spectratyping. Correlation with immune status. *J Immunol.* 1994;152(10):5109-5119.
- Fallen PR, et al. Factors affecting reconstitution of the T cell compartment in allogeneic haematopoietic cell transplant recipients. *Bone Marrow Transplant.* 2003;32(10):1001-1014.
- Bosch M, Khan FM, Storek J. Immune reconstitution after hematopoietic cell transplantation. *Curr Opin Hematol.* 2012;19(4):324-335.
- Cohen JL, Trenado A, Vasey D, Klatzmann D, Salomon BL. CD4⁺CD25⁺ immunoregulatory T cells: new therapeutics for graft-versus-host disease. *J Exp Med.* 2002;196(3):401-406.
- Hoffmann P, Ermann J, Edinger M, Fathman CG, Strober S. Donor-type CD4⁺CD25⁺ regulatory T cells suppress lethal acute graft-versus-host disease after allogeneic bone marrow transplantation. *J Exp Med.* 2002;196(3):389-399.
- Trenado A, et al. Recipient-type specific CD4⁺CD25⁺ regulatory T cells favor immune reconstitution and control graft-versus-host disease while maintaining graft-versus-leukemia. *J Clin Invest.* 2003;112(11):1688-1696.
- Mielke S, et al. Reconstitution of FOXP3⁺ regulatory T cells (Tregs) after CD25-depleted allotransplantation in elderly patients and association with acute graft-versus-host disease. *Blood.* 2007;110(5):1689-1697.
- Wolf D, et al. Regulatory T cells in the graft and the risk of acute graft-versus-host disease after allogeneic stem cell transplantation. *Transplantation.* 2007;83(8):1107-1113.
- Nguyen VH, et al. The impact of regulatory T cells on T cell immunity following hematopoietic cell transplantation. *Blood.* 2008;111(2):945-953.
- Brunstein CG, et al. Infusion of ex vivo expanded T regulatory cells in adults transplanted with umbilical cord blood: safety profile and detection kinetics. *Blood.* 2011;117(3):1061-1070.
- Gaidot A, et al. Immune reconstitution is preserved in hematopoietic stem cell transplantation coadministered with regulatory T cells for GVHD prevention. *Blood.* 2011;117(10):2975-2983.
- Nguyen VH, et al. In vivo dynamics of regulatory T cell trafficking and survival predict effective strategies to control graft-versus-host disease following allogeneic transplantation. *Blood.* 2007;109(6):2649-2656.
- Gudmundsdottir H, Wells AD, Turka LA. Dynamics and requirements of T cell clonal expansion in vivo at the single-cell level: effector function is linked to proliferative capacity. *J Immunol.* 1999;162(9):5212-5223.
- Gudmundsdottir H, Turka LA. A closer look at homeostatic proliferation of CD4⁺ T cells: costimulatory requirements and role in memory formation. *J Immunol.* 2001;167(7):3699-3707.
- Fazekas de St Groth B, Smith AL, Koh WP, Girgis L, Cook MC, Bertolino P. Carboxyfluorescein diacetate succinimidyl ester and the virgin lymphocyte: a marriage made in heaven. *Immunol Cell Biol.* 1999;77(6):530-538.
- Kieper WC, et al. Recent immune status determines the source of antigens that drive homeostatic T cell expansion. *J Immunol.* 2005;174(6):3158-3163.
- Do JS, et al. Both exogenous commensal and endogenous self antigens stimulate T cell proliferation under lymphopenic conditions. *Cell Immunol.* 2012;272(2):117-123.
- Winstead CJ, Fraser JM, Khoruts A. Regulatory

- CD4⁺CD25⁺Foxp3⁺ T cells selectively inhibit the spontaneous form of lymphopenia-induced proliferation of naive T cells. *J Immunol.* 2008;180(11):7305–7317.
24. Boyman O, Kovar M, Rubinstein MP, Surh CD, Sprent J. Selective stimulation of T cell subsets with antibody-cytokine immune complexes. *Science.* 2006;311(5769):1924–1927.
25. Hagen KA, Moses CT, Drasler EF, Podetz-Pedersen KM, Jameson SC, Khoruts A. A role for CD28 in lymphopenia-induced proliferation of CD4 T cells. *J Immunol.* 2004;173(6):3909–3915.
26. Cederbom L, Hall H, Ivars F. CD4⁺CD25⁺ regulatory T cells down-regulate co-stimulatory molecules on antigen-presenting cells. *Eur J Immunol.* 2000;30(6):1538–1543.
27. Misra N, Bayry J, Lacroix-Desmazes S, Kazatchkine MD, Kaveri SV. Cutting edge: human CD4⁺CD25⁺ T cells restrain the maturation and antigen-presenting function of dendritic cells. *J Immunol.* 2004;172(8):4676–4680.
28. Oderup C, Cederbom L, Makowska A, Cilio CM, Ivars F. Cytotoxic T lymphocyte antigen-4-dependent down-modulation of costimulatory molecules on dendritic cells in CD4⁺CD25⁺ regulatory T cell-mediated suppression. *Immunology.* 2006;118(2):240–249.
29. Wing K, et al. CTLA-4 control over Foxp3⁺ regulatory T cell function. *Science.* 2008;322(5899):271–275.
30. Cretny E, et al. The transcription factors Blimp-1 and IRF4 jointly control the differentiation and function of effector regulatory T cells. *Nat Immunol.* 2011;12(4):304–311.
31. Bachmann MF, Köhler G, Ecabert B, Mak TW, Kopf M. Lymphoproliferative disease in the absence of CTLA-4 is not T cell autonomous. *J Immunol.* 1999;163(3):1128–1131.
32. Grohmann U, et al. CTLA-4-Ig regulates tryptophan catabolism in vivo. *Nat Immunol.* 2002;3(11):1097–1101.
33. Fallarino F, et al. Modulation of tryptophan catabolism by regulatory T cells. *Nat Immunol.* 2003;4(12):1206–1212.
34. Uytendhoeve C, et al. Evidence for a tumoral immune resistance mechanism based on tryptophan degradation by indoleamine 2,3-dioxygenase. *Nat Med.* 2003;9(10):1269–1274.
35. Fazekas de St Groth B, Patten PA, Ho WY, Rock EP, Davis MM. An analysis of T cell receptor-ligand interaction using a transgenic antigen model for T cell tolerance and T cell receptor mutagenesis. In: Alt FW, Vogel HJ, eds. *Molecular Mechanisms Of Immunological Self-Recognition*. San Diego, California, USA: Academic Press; 1992:123–127.
36. Seder RA, Paul WE, Davis MM, Fazekas de St Groth B. The presence of interleukin 4 during in vitro priming determines the lymphokine-producing potential of CD4⁺ T cells from T cell receptor transgenic mice. *J Exp Med.* 1992;176(4):1091–1098.
37. Lahl K, et al. Selective depletion of Foxp3⁺ regulatory T cells induces a scurfy-like disease. *J Exp Med.* 2007;204(1):57–63.
38. Kim JM, Rasmussen JP, Rudensky AY. Regulatory T cells prevent catastrophic autoimmunity throughout the lifespan of mice. *Nat Immunol.* 2007;8(2):191–197.
39. Winstead CJ, et al. CD4⁺CD25⁺Foxp3⁺ regulatory T cells optimize diversity of the conventional T cell repertoire during reconstitution from lymphopenia. *J Immunol.* 2010;184(9):4749–4760.
40. Min B, Yamane H, Hu-Li J, Paul WE. Spontaneous and homeostatic proliferation of CD4 T cells are regulated by different mechanisms. *J Immunol.* 2005;174(10):6039–6044.
41. Cozzo C, Larkin J 3rd, Caton AJ. Self-peptides drive the peripheral expansion of CD4⁺CD25⁺ regulatory T cells. *J Immunol.* 2003;171(11):5678–5682.
42. Merad M, et al. Langerhans cells renew in the skin throughout life under steady-state conditions. *Nat Immunol.* 2002;3(12):1135–1141.
43. Bogunovic M, et al. Identification of a radio-resistant and cycling dermal dendritic cell population in mice and men. *J Exp Med.* 2006;203(12):2627–2638.
44. Taylor PA, Lees CJ, Blazar BR. The infusion of ex vivo activated and expanded CD4⁽⁺⁾CD25⁽⁺⁾ immune regulatory cells inhibits graft-versus-host disease lethality. *Blood.* 2002;99(10):3493–3499.
45. Vogtenhuber C, et al. Constitutively active Stat5b in CD4⁺ T cells inhibits graft-versus-host disease lethality associated with increased regulatory T cell potency and decreased T effector cell responses. *Blood.* 2010;116(3):466–474.
46. Gerold KD, Zheng P, Rainbow DB, Zerneck A, Wicker LS, Kissler S. The soluble CTLA-4 splice variant protects from type 1 diabetes and potentiates regulatory T cell function. *Diabetes.* 2011;60(7):1955–1963.
47. Qureshi OS, et al. Trans-endocytosis of CD80 and CD86: a molecular basis for the cell-extrinsic function of CTLA-4. *Science.* 2011;332(6029):600–603.
48. Kojima A, Tanaka-Kojima Y, Sakakura T, Nishizuka Y. Spontaneous development of autoimmune thyroiditis in neonatally thymectomized mice. *Lab Invest.* 1976;34(6):550–557.
49. Sakaguchi S, Sakaguchi N. Thymus and autoimmunity: capacity of the normal thymus to produce pathogenic self-reactive T cells and conditions required for their induction of autoimmune disease. *J Exp Med.* 1990;172(2):537–545.
50. Sakaguchi S, Sakaguchi N. Organ-specific autoimmune disease induced in mice by elimination of T cell subsets: V. neonatal administration of cyclosporin A causes autoimmune disease. *J Immunol.* 1989;142(2):471–480.
51. Sakaguchi S, et al. Induction of autoimmune disease in mice by germline alteration of the T cell receptor gene expression. *J Immunol.* 1994;152(3):1471–1484.
52. Kanakry CG, et al. Aldehyde dehydrogenase expression drives human regulatory T cell resistance to posttransplantation cyclophosphamide. *Sci Transl Med.* 2013;5(211):211ra157.
53. D'Addio F, et al. Prolonged, low-dose anti-thymocyte globulin, combined with CTLA4-Ig, promotes engraftment in a stringent transplant model. *PLoS One.* 2013;8(1):e53797.
54. Luznik L, Jones RJ, Fuchs EJ. High-dose cyclophosphamide for graft-versus-host disease prevention. *Curr Opin Hematol.* 2010;17(6):493–499.
55. Gurkan S, et al. Immune reconstitution following rabbit antithymocyte globulin. *Am J Transplant.* 2010;10(9):2132–2141.
56. Alpdogan O, et al. IL-7 enhances peripheral T cell reconstitution after allogeneic hematopoietic stem cell transplantation. *J Clin Invest.* 2003;112(7):1095–1107.
57. Guimond M, et al. Interleukin 7 signaling in dendritic cells regulates the homeostatic proliferation and niche size of CD4⁺ T cells. *Nat Immunol.* 2009;10(2):149–157.
58. Alpdogan O, et al. Administration of interleukin-7 after allogeneic bone marrow transplantation improves immune reconstitution without aggravating graft-versus-host disease. *Blood.* 2001;98(7):2256–2265.
59. Gameiro SR, Caballero JA, Higgins JP, Apelian D, Hodge JW. Exploitation of differential homeostatic proliferation of T cell subsets following chemotherapy to enhance the efficacy of vaccine-mediated antitumor responses. *Cancer Immunol Immun.* 2011;60(9):1227–1242.
60. Baba J, et al. Depletion of radio-resistant regulatory T cells enhances antitumor immunity during recovery from lymphopenia. *Blood.* 2012;120(12):2417–2427.
61. Yao X, et al. Levels of peripheral CD4⁺FoxP3⁺ regulatory T cells are negatively associated with clinical response to adoptive immunotherapy of human cancer. *Blood.* 2012;119(24):5688–5696.
62. Edinger M, et al. CD4⁺CD25⁺ regulatory T cells preserve graft-versus-tumor activity while inhibiting graft-versus-host disease after bone marrow transplantation. *Nat Med.* 2003;9(9):1144–1150.
63. Arkwright PD, Abinun M, Cant AJ. Autoimmunity in human primary immunodeficiency diseases. *Blood.* 2002;99(8):2694–2702.
64. Spanopoulou E, et al. Functional immunoglobulin transgenes guide ordered B-cell differentiation in Rag-1-deficient mice. *Genes Dev.* 1994;8(9):1030–1042.
65. Shinkai Y, et al. RAG-2-deficient mice lack mature lymphocytes owing to inability to initiate V(D)J rearrangement. *Cell.* 1992;68(5):855–867.
66. Chambers CA, Cado D, Truong T, Allison JP. Thymocyte development is normal in CTLA-4-deficient mice. *Proc Natl Acad Sci U S A.* 1997;94(17):9296–9301.
67. Lahl K, Sparwasser T. In vivo depletion of FoxP3⁺ Tregs using the DEREK mouse model. *Methods Mol Biol.* 2011;707:157–172.
68. Cooke KR, et al. An experimental model of idiopathic pneumonia syndrome after bone marrow transplantation: I. The roles of minor H antigens and endotoxin. *Blood.* 1996;88(8):3230–3239.